

# A variational model for plastic slip and its regularization *via* $\Gamma$ –convergence.

LUIGI AMBROSIO

Scuola Normale Superiore  
Piazza dei Cavalieri 7, I56127 Pisa, Italy

ANTOINE LEMENANT

Centro di Ricerca Matematica Ennio De Giorgi  
Piazza dei Cavalieri 3, I56127 Pisa, Italy

GIANNI ROYER-CARFAGNI

Università degli Studi di Parma  
Viale G. Usberti 181/A, I43100 Parma, Italy

July 27, 2011

## Abstract

A variational model is presented able to interpret the onset of plastic deformations, here modeled as displacement jumps occurring along slip surfaces at constant yielding stress. The corresponding strain energy functional, leading to a *free-discontinuity* problem set in the space of *SBV* functions, is then approximated by a sequence of *regularized* elliptic functionals following the seminal work in Ambrosio-Tortorelli (1990) within the framework of  $\Gamma$ –convergence. Comparisons between the results obtainable with the free-discontinuity model and its regularized approximation, in terms of stability of the pure elastic phase, irreversibility of plastic slip and response under unloading, are presented, in general, for the 2-D case of antiplane shear and exemplified, in particular, for the 1-D case.

KEYWORDS: Plasticity; plastic slip; variational model; free-discontinuity problem;  $\Gamma$ –convergence; cohesive fracture.

MATHEMATICS SUBJECT CLASSIFICATIONS (2000): 28A75, 35R35, 74G65, 74R05, 74R10, 74R20.

## 1 Introduction

The term “plasticity” usually refers to the behavior of materials which undergo irreversible deformations without fracture or damage, and the transition from elastic to plastic behavior

is usually referred to as *yield*. There are several mathematical description of plasticity [42] that are essentially *bulk* theories, because they assume that the plastic part of the deformation can be described by sufficiently *regular* mappings from the reference configuration of the body. These obey to non-linear, non-integrable equations, to describe the set of changes on strain and stress with respect to a previous state and a small increase of deformation, presented in the form of yield criterion, flow rule, hardening law and stress-strain relation. A case of particular interest because of its simplicity is that of an *ideal* plastic material, for which the rate of hardening is assumed to be zero so that the body may undergo unlimited irreversible deformations at constant *yielding* stress.

However, experimental observations have provided evidence that when ductile solids are deformed sufficiently into the plastic range, the surface of a locally yielded zone must run along a surface of slip, where the deformation highly localizes in the form of coarse bands, usually following the directions of maximum shear. Such shear bands, once formed, persist and the subsequent deformation correspondingly presents high gradients similar to displacement jumps. Localization in the form of shear bands usually represents the preferential pre-failure deformation mode not only of ductile metals [45], but also of natural rocks [41], granular materials [53] and other substances [46].

The aim of this paper is to present a model to characterize and interpret the strain localization in the form of *coarse shear bands*. The mathematical characterization of this phenomenon may follow two different rationales. The process may be considered an instability that can be predicted in terms of the pre-localization constitutive relations of the material [8]: critical conditions are sought at which a bifurcation occurs from homogeneous or smoothly varying deformation into a highly concentrated shear band mode. The alternative hypothesis consists in assuming that, at a certain stage of the load history, an alternative competing physical mechanism of deformation comes into play that rapidly affects the material strength: in this case, the pre-localization constitutive relationships cannot be continued analytically at the critical point and they provide no basis for prediction of localization. This transition is usually triggered by an irreversible event, such as the rupture of an anchoring ligament.

Here, this second approach is followed. In particular, plastic strain localization is assumed to be consequent to the breaking free of the potential sliding surfaces from a pinning obstacle, after which sliding at constant yielding stress can occur. The necessity of overcoming an energetic barrier to unpin a slip surface is of basilar importance for the model. From the point of view of mathematical description, if this barrier goes to zero no pre-localization (elastic) stage would be possible in the body, which would thus present no resistance against a structured deformation composed of micro-slips. Moreover, the energetic barrier implies a strain-softening macroscopic response, associated with the drop of the shear resistance from the peak to the residual value. The experimental evidence also gives reasons for the presence of the unpinning energy. In the case of mild steel, its contribution is crucial for the orderly formation of shear bands and explains the transition from an upper to a lower yield point [31]; for rocks and geomaterials, one may mention the famous paper by Palmer and Rice [43] where, in order to model the growth of localized shear bands in the progressive failure of over-consolidated clay or sand as seen in the experiments, the authors had to as-

sume an energetic competition analogous to that of fracture mechanics to derive conditions for the propagation of the tip of a concentrated shear band into the sound material.

If one associates the plastic part of the deformation with the discontinuities in the displacement field due to plastic slips, either at the microscopic or macroscopic level, and assumes the presence of an unpinning energy, the mathematical description of the phenomenon of plastic yielding presents strict similarities with fracture mechanics. Indeed, the unpinning energy plays the same role of fracture energy, but there is a substantial difference. In brittle fracture, once that a certain amount of energy has been paid to create new fracture surface, the crack lips can depart from one another with no further energy consumption; on the other hand, the plastic slip occurs at certain non-zero stress level (defined by the yielding stress), which approximately remains constant during the yielding phase and, consequently, some work has to be expended to increase the amount of slip. A link between the two theories is provided by the approach by Dugdale [26], that accounts for plasticity at the crack tips or, more in general, by Barenblatt's cohesive crack model [7]. The possibility of embracing the phenomena of fracture and yielding within a unified approach has also been explored by Del Piero [23], who was able to reproduce the peculiar features of these apparently different-in-type material responses by simply varying the form of the constitutive law that regulates the intensity of the cohesive surface forces as a function of the crack opening displacement. However, the difference between cohesive fracture and plastic gliding is that in the former the cohesive forces bridging the crack lips are usually decreasing functions of the crack opening displacement tending to the null value, whereas in the latter the yield stress is assumed to remain practically constant during localized gliding. Consequently, infinite energy would be necessary to produce a complete separation of the body, but this is because this interpretation of plasticity fits only to the first pre-failure stages of plastic flow and neglects the final stage eventually leading to fracture.

The purpose here is to present a variational formulation of the phenomenon of plastic slip, which extends to the case of plasticity the approach first introduced by Francfort and Marigo for the case of brittle fracture. In [28], the authors proposed a variational model of quasistatic crack evolution through the minimization of an energy functional composed of a bulk term, i.e., the strain of the sound material, and a surface energy term *à la* Griffith, and by adding proper irreversibility conditions for crack opening. The model now presented is similar but substantially different because of the addition of a further surface energy term, interpreting the work to be consumed to increase plastic gliding at constant yielding stress. This model is also a particular two-dimensional extension of the general theory proposed for example in [25] for the one-dimensional case.

From a mathematical point of view, our main result consists in the regularization of the proposed variational formulation of plastic yielding, leading to a *free-discontinuity problem*, with an elliptic two-field functional, where one field is representative of the macroscopic displacement in the body, while the other one is an *order parameter*, of the type commonly employed to describe phenomena of phase transition, which is 0 in the sound state of the body and 1 in the yielded state. Therefore, this regularized theory lays in the class of *phase-field models*, where the regularization is obtained through the introduction of gradient terms, that induce a smooth transition between the values of the order parameter on both sides of

the interface [38]. A particularly interesting phase-field model of fracture has been recently proposed in [34], which also contains laws of crack-tip motion, stability analysis, generalized Eshelby-Rice integrals and an exhaustive list of relevant references.

When compared with the case of brittle fracture, the proposed regularized functional represents the natural extension to the case of plasticity of the regularized variational approximation of brittle fracture proposed in [11] for the functional of [28]. In that case, the approximation was corroborated by a  $\Gamma$ -convergence result. In fact, in [11] the regularized functional was characterized by a parameter indicated by  $\varepsilon$  and a direct use of the Ambrosio-Tortorelli [3] weak formulation of the Mumford-Shah functional in problems of image-segmentation, allowed to verify for the case of antiplane shear<sup>1</sup> that, as  $\varepsilon \rightarrow 0$ , the elliptic functional  $\Gamma$ -converges to the parent Griffith-like functional of [28]. Here, we extend this result by proving the  $\Gamma$ -convergence of the proposed regularized elliptic two-field functional towards the free-discontinuity variational problem for plastic yielding. Other approaches to plasticity loosely related to the one here considered were proposed in [12] for a model of Hencky's plasticity and in [1], but for approximating regularized energy-functionals with linear growth in the displacement gradient, that thus  $\Gamma$ -converge to functionals settled in the space BV of functions of bounded variation. Here, on the other hand, the leading term in the energy of the displacement gradient is quadratic and the resulting  $\Gamma$ -limit is defined in the class SBV of special functions of bounded variation.

This paper can be read at two levels, one more physical, the other one more mathematical. Section 2 recalls experimental results that evidence the localization of plastic flow in coarse bands and the importance of the energetic barrier to unpin glide surfaces. Section 3 illustrates the model and its variational characterization. The main result of  $\Gamma$ -convergence is contained in Section 4, which is the most substantial from a mathematical point of view but self-contained. Comparisons between the results obtainable with the free-discontinuity model and its regularized approximation are developed for the 1-D case in Section 5.

## 2 The localization of plastic flow

The purpose of this Section is twofold: to illustrate the experimental evidence of the formation of shear bands in ductile solids and to give reasons why the onset of such mechanism from a preceding state of strain, sufficiently smooth and regular, should arise from the breaking free of potential glide surfaces from pinning obstacles at the price of energy consumption.

As a matter of fact, any irreversible plastic flow in metals is the consequence of structured deformations in the form of microslips. To illustrate, fig. 1 shows a uniaxially stretched copper-aluminum bar, from which it is evident that the plastic part of the elongation is due to slips concentrated in bands, a few microns wide, spaced throughout the

---

<sup>1</sup>Later on, the  $\Gamma$ -convergence result was demonstrated also in the vectorial case for the elastic energy by Chambolle [14] and for a certain class of general integrands by Focardi [27]. An exhaustive list of references for this kind of problems can be found in [4].

specimen [39]. Since a representative volume element is likely to contain a great number of bands, the gross response of the material can be described by regular functions taking a *smear*ed view of the phenomenon, as in the traditional mathematical theory of plasticity. This method is perfectly adequate to describe the *macroscopic* consequences of plastic deformation.

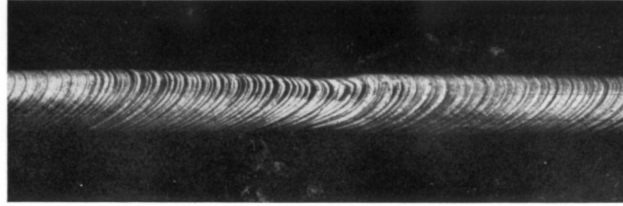


Figure 1: Extended copper-aluminum single crystal (experiment by Elam [39]).

These bands are usually referred to as Lüders' or flow lines. Lüders' bands represent the *microscopic* mechanism of plasticity that can be explained, at the atomic level, in terms of the theory of dislocation (see, e.g., [17, Sec. 13]) as realized, roughly simultaneously, by Orowan, Polanyi and Taylor already in 1934 [39]. Gliding along such bands needs to be activated by overcoming an energetic barrier and this is why metallic alloys show a pure elastic phase when the strain is relatively small, while a sharp yield point marks the onset of the plastic phase. There is a classical explanation for this phenomenon. In ferrous alloys solute atoms, which are able to migrate through the crystal under the action of thermal fluctuations, will, in the presence of an inhomogeneous field such as the stress field of a dislocation, drift towards those places where their energy state is lowest. Thus, the starting scenario of an unyielded portion of an alloy is the segregation of solute atoms around stationary dislocations. Since the migration of solute atoms takes much longer than the movement of a dislocation, in the presence of an external stress field, dislocations will initially remain anchored (pinned) to the surrounding atmosphere produced by the solute atoms. If a long enough time is allowed during the tests for the migration of solute atoms to occur, creep effects may become important. However, if the loading speed is high enough to allow discounting such an effect, the material could exist in either of two conditions: in the first, the unyielded or strain-aged condition, the dislocations are anchored and deformation is purely elastic; in the second, the overstrained condition, dislocations are free to move under applied stress to produce plastic deformations. In order break the anchoring link of a dislocation, a certain amount of energy has to be consumed. It is this energetic balance that is responsible of the transition from an upper to a lower yield point that is evident in the experiments, interpreted in [31] through a simple but effective mechanical model, consisting in a particular arrangement of spring-dashpot units [31].

However, when the plastic deformation progresses, ductile metals often present an abrupt flow, concentrated within certain single layers or surfaces. The appearance of such layers represents the *macroscopic* manifestation of strain localization, a phenomenon that needs *ad hoc* modeling. Such mechanism is certainly associated with dislocation movements,

but other phenomena create preferential paths along thin glide layers. For example, the formation of macro-bands, as showed in many images by Nadai [39], is certainly favored by initial stress concentrations in the elastic regime, such as those produced by notches and holes. Such bands, sometimes referred to as *coarse bands* or *superbands*, usually progress in a crack-like propagation, rather than being the consequence of a sudden bifurcation from a uniform deformation field.

It should be mentioned that coarse bands appear both in metallic single crystal and polycrystal, but the mechanism of formation is slightly different for the two cases. In single crystals the macro-glide can be activated by necking [5] or by “cross slip” of Lüders’ bands [44]. Pre-straining the crystal may also produce the formation of coarse bands to near zero initial rates of hardening [52], and, in general, the slip in the coarse slip zone is constant and without apparent weakening. On the other hand, the coarse localization occurring in ductile polycrystals and structural alloys is usually triggered by nucleation of micro-holes from brittle microcracking or decohesion of inclusions. In early experiments on AISI 4340 alloy recorded in [18], large inclusions nucleated voids that initially appeared as a collection of small voids (fig. 2a), similar to a “void sheet”. As the strain is increased, the small void coalesce through a band of localized shearing (fig. 2b), whose progression presents strict similarities with a crack opening because it is associated with an energy consumption. Indeed, the localization mechanism also influences the response of sharply pre-cracked metals [33], because the advancement of the crack tip is due to its coalescence with a neighboring voids, when the stress concentration reaches a critical threshold.

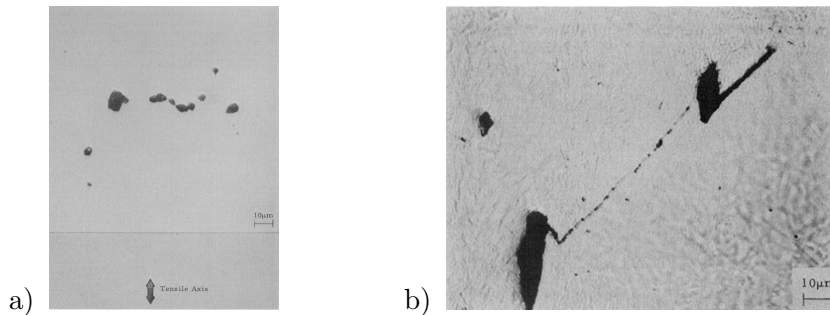


Figure 2: a) Void sheet nucleated from inclusion decohesion in an AISI 4340 steel strained plastically; b) coalescence of voids by a band of localized shearing.

The phenomenon of plastic localization in pure shear has also been evidenced in cylindrical bars of high-strength AISI 4340 steel under large torsional strains [49]. More recent experiments on mild steel bars [9] have given similar results. The onset of plastic deformation in the twisted bar is associated with the formation of thin Lüders-like bands following the transversal direction of the highest shearing stress but, as the twist angle is augmented, single coarse slip bands form in longitudinal direction where shear deformation is concentrated. Figs. 3a and 3b represent, at two different scale of magnification, a surface portion of the bar, where the Lüders-like bands are slightly inclined on the horizontal and the coarse slip bands follow a helix wrapping around the cylindrical bar because of the permanent plas-

tic twist. The mismatch of the transversal bands, evident in fig. 3b, indicates that once the longitudinal coarse slip has been nucleated, plastic deformation continues to concentrate there as the twisting angle is augmented. The eventual stage is the progressive failure of the bar along the coarse plastic band (ductile fracture). This is evidenced in fig. 3c that shows a SEM photograph of the transversally cut bar, where the incipient fracture appears like a groove that certainly induces a stress concentration. Also for this case the formation of coarse bands can be explained if one assumes that an unpinning energy has to be overcome to allow the transition from the transversal to the longitudinal shear deformation [9].

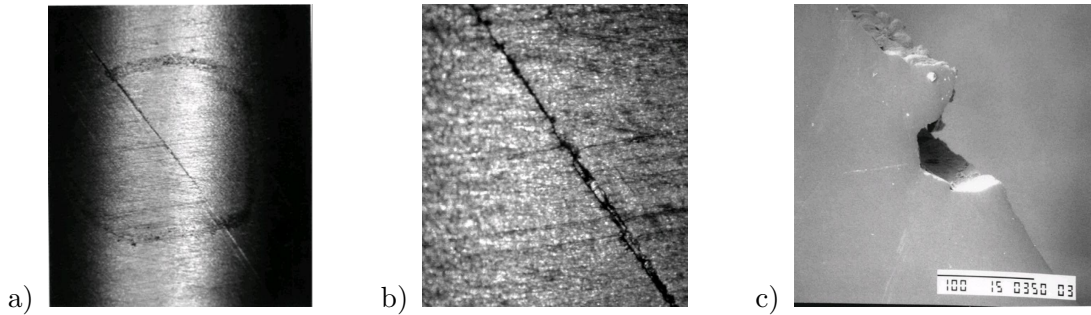


Figure 3: a) Lüders-like bands (pseudo-horizontal) and coarse slip bands (inclined) on the lateral surface of a highly rotated bar of mild steel. b) Magnification of the coarse slip band, with evidence of longitudinal slip mode. c) Scanning Electron Microscope photograph of a cross section of the bar with evidence of the longitudinal coarse slip band and incipient ductile fracture [9].

It should also be mentioned that localization instabilities may also be facilitated by geometric effects. For example, wide flat bars obtained from thin metal sheets when tested in tension do not break in a surface which is perpendicular to the direction of tension, but along an oblique plane where shear deformations localize. Fig. 4a shows an image from a classical experiment by Körber and Siebel [36]. This mechanism of plastic deformation is essentially due to the width of the specimens, that facilitates the mechanics evidenced in fig. 4b. Judged as three-dimensional problems, these are distinctly different from the aforementioned cases because they involve “geometric” as opposed to “material” instability, but when modeled as two-dimensional continua, the problem of localization may be treated by considering that the 3-D instability is associated with the surmounting of an energetic barrier that in the 2-D case is equivalent to the assumption of an unpinning energy barrier to nucleate and propagate the coarse band [45].

Another important class of materials whose stability response is characterized by marked strain localization is represented by geomaterials. It is common evidence that sliding of great mass of overconsolidated clay occurs along very narrow slip surfaces [32] and, indeed, an engineering way of assessing the stability of slopes consists in assuming a constitutive equation for sliding along the slip surface, and in verifying that the internal work for downslope mass movement is greater than the work of the applied loads. Localization occurs as well in sand specimens [47]. Also natural rock especially when under compressive stresses shows

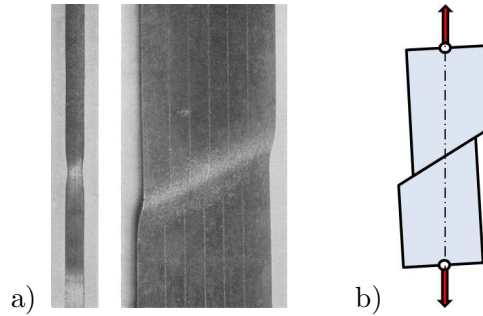


Figure 4: a) Necking and plastic strain localization along transversal coarse band in a flat bar [36]. b) Geometric effect in the mechanism of plastic deformation.

examples of strain localization, usually referred to as faulting. Here the inelastic deformation is due to frictional sliding on closed microcracks and progressive enlargement of the microcrack network through local fissuring; the final macroscopic fault links a large number of such microcracks, although their individual directions of growth do not coincide with that of the final fault. This mechanism is always associated with energy consumption of the same form of classical fracture mechanics. At the much larger length-scale of geological masses, sharp faults with associated slip of a few millimeters or centimeters width are abundant in sandstones, preceding the development of large faults with displacements of several meters or tens of meters. The small faults usually contain no-surfaces of discontinuity, rather they occur as deformation bands about one millimeter thick and tens or hundreds of meters long, across which the slip is distributed [6].

The examples just illustrated show that plastic gliding along coarse bands is an abrupt phenomenon characterized by the breaking free of the potential sliding surfaces from a pinning obstacle. One of the first models where a mechanism of this type has been taken into account is that by Palmer and Rice [43], who considered stress intensity factors,  $J$ -integral and energy balance to follow the propagation of the tip of a concentrated shear band. Their approach assumed a gradual decay of shear resistance within the end zone of the shear band, from peak to residual values, with increasing relative sliding displacement. This implies that the progression of a shear bands eventually leads to the neat separation (fracture) of the material. Further applications of the linear elastic fracture mechanics concepts of energy balance and process zone approaches have been considered in [48] for more general types of soil than that considered in [43], by assuming that once local deformations reach conditions for localization, the constitutive relations for continuum-like deformation are suspended in favor of a relation between tractions and relative displacements of the surfaces of the zone of localization (presumed thin).

More recently, Bigoni and Dal Corso [8] have addressed new questions for the mechanisms of coarse slip-band propagation, here considered as an instability phenomenon, that can be summarized as follows. A shear band tip involves a strong stress concentration that drives its growth, but this occurs quasi-statically in mode II along a straight line, whereas this is not observed in the akin problem of crack growth. The authors were able

to demonstrate that shear bands are the preferential failure mode for quasi-statically deformed ductile materials by proposing analytical solutions to investigate the state of stress and growth conditions for a shear band of finite-length in a prestressed ductile material. The corresponding deformation becomes aligned coaxial with the shear band, thus confirming the strong tendency towards rectilinear propagation. However, the energy release rate blows up to infinity when reaching the elliptic boundary concluding that the propagation becomes “unrestrainable”, a result confirming that shear bands are the preferential near-failure deformation modes.

In the model that will be considered here, plasticity is represented by inelastic gliding along slip shear bands. The shear stress bridging the two contact surfaces is supposed, in the simplest case, to remain constant and equal to the yielding limit. A key point is that, in order to break free any potential glide surface, an “unpinning” energy per unit area has to be consumed, so that an elastic release from the other parts of the body remaining elastic is associated to the onset of plasticity. This unpinning energy has to be paid only *once*, so that relative movements of the gliding surfaces after unpinning can occur, either forward or backward (unloading), with no other energy consumption than that corresponding to the work to overcome the yielding stress.

Equilibrium configurations are sought as minimizers of an energy functional, establishing an energetic competition among three terms: the *elastic bulk energy*, stored in the sound material portions; the *surface unpinning energy*, interpreting the work to be paid to break free the slip surface; the *surface plastic energy*, corresponding to the shear resistance of contiguous sliding lips. Proper conditions are added to account for the irreversibility of unpinning energy release and plastic work.

### 3 The variational formulation of plasticity

The elastic-plastic body that will be considered here is amenable of undergoing extremely high strains concentrated on layers of infinitesimal thickness that can be modeled as discontinuities in the component of displacement tangential to the surfaces of slip. Since the variational problem requires that the space of functions for the deformation field allows for this kind of discontinuities, the most appropriate choice for this task is the space of functions of Special Bounded Variation, briefly referred to as SBV. For the sake of completeness, before presenting the energy functional, we recall first some classical definitions and properties of the space *SBV* as introduced in [21] (see also [2] for a survey on the theory).

#### 3.1 Short review on SBV functions

In the sequel  $N$  will denote the dimension of the ambient space. For any open set  $\Omega \subset \mathbb{R}^N$ , the space  $BV(\Omega)$  is the class of all functions  $u \in L^1_{loc}(\Omega, \mathbb{R})$  such that  $Du$  (the derivative of  $u$  in the distributional sense) is a finite measure. A real  $z \in \mathbb{R}$  is an approximate limit for

$u$  at point  $x$  if

$$\lim_{\rho \rightarrow 0} \frac{1}{|B(x, \rho)|} \int_{B(x, \rho)} |u(y) - z| dy = 0.$$

The set  $S_u$  of points where this property does not hold is called the *approximate discontinuity set* of  $u$ . For any  $x \in \Omega \setminus S_u$  the approximate limit of  $u$  at  $x$  will be denoted  $\tilde{u}(x)$ .

A remarkable result of Federer and Vol'pert (see [2, Th. 3.78.]) says that when  $u \in BV(\Omega)$ , then  $S_u$  is countably  $\mathcal{H}^{N-1}$ -rectifiable and  $D^s u$  (the singular part of  $Du$  with respect to  $\mathcal{L}^N$  in the Radon-Nikodym decomposition  $Du = D^a u + D^s u$ ) restricted to  $S_u$  is absolutely continuous with respect to  $\mathcal{H}^{N-1}$ . We will say that  $u \in SBV(\Omega)$  when  $D^s u$  is actually *concentrated* on  $S_u$ .

The density of regular part  $D^a u$  of  $Du$  with respect to  $\mathcal{L}^N$ , denoted by  $\nabla u$ , coincides  $\mathcal{L}^N$ -a.e. with the *approximate differential* of  $u$  (see [2, Th. 3.83.]). Recall that  $u$  is approximately differentiable at  $x$  if there exists a vector  $\nabla u(x)$  such that

$$\lim_{\rho \rightarrow 0} \frac{1}{|B(x, \rho)|} \int_{B(x, \rho)} \frac{|u(y) - \tilde{u}(x) - \nabla u(x) \cdot (y - x)|}{\rho} dy = 0.$$

In the sequel we will also use the notion of *trace* of  $u$  on the singular set  $S_u$ . Since  $S_u$  is rectifiable, one can fix an orientation  $\nu_u : S_u \rightarrow S^{N-1}$  in such a way that for  $\mathcal{H}^{N-1}$ -a.e.  $x \in S_u$  the approximate tangent space to  $S_u$  at  $x$  is orthogonal to the vector  $\nu_u(x)$ . Then for any  $x \in S_u$  and  $\rho > 0$  we define  $B(x, \rho)^+ := B(x, \rho) \cap \{y; \langle y, \nu_u(x) \rangle \geq 0\}$  and  $B(x, \rho)^- := B(x, \rho) \cap \{y; \langle y, \nu_u(x) \rangle \leq 0\}$ . For  $\mathcal{H}^{N-1}$ -a.e.  $x \in S_u$ , Theorem 3.77. of [2] provides the existence of traces  $u^+(x)$  and  $u^-(x)$  satisfying

$$\lim_{\rho \rightarrow 0} \frac{1}{|B(x, \rho)^\pm|} \int_{B(x, \rho)^\pm} |u(y) - u^\pm(x)| dy = 0.$$

The set of points  $x \in S_u$  where  $u^\pm(x)$  exist is called the *jump set* and is denoted by  $J_u$ . It can be shown that  $\mathcal{H}^{N-1}(S_u \setminus J_u) = 0$  and for  $x \in J_u$  the quantity  $(u^+(x) - u^-(x))$  is called the *jump* of  $u$  at point  $x$ , which sign depends on the orientation of  $S_u$ . Moreover for any  $u \in SBV(\Omega)$  the representation

$$D^s u = (u^+ - u^-) \nu_u \mathcal{H}^{N-1} \llcorner S_u,$$

holds.

### 3.2 The variational model in antiplane shear

Let now  $\Omega$  denote a bounded connected open set of  $\mathbb{R}^N$ . Although the mathematical formulation fits any finite value of  $N$ , the main situation that will be considered here is that of an elastic body under antiplane shear for which we set  $N = 2$ . Given an orthonormal Cartesian frame  $(O; \mathbf{e}_1, \mathbf{e}_2, \mathbf{e}_3)$ , the body is a right cylinder with generator parallel to  $\mathbf{e}_3$ , cross section  $\Omega$  and bases at  $x_3 = \pm h/2$ , so that it identifies with the Cartesian product  $\mathcal{B} = \Omega \times (-h/2, h/2)$  and a typical point is  $\mathbf{z} = \mathbf{x} + x_3 \mathbf{e}_3$ , with  $(\mathbf{x}, x_3) \in \Omega \times (-h/2, h/2)$ . In antiplane shear, the displacement field is assumed to be of the form  $\mathbf{u}(\mathbf{z}) = u(\mathbf{x}) \mathbf{e}_3$ , so

that  $u : \Omega \rightarrow \mathbb{R}$  is the displacement component in the direction perpendicular to the plane of interest, while the in-plane components equal to zero. Let  $\nabla u = \partial_1 u \mathbf{e}_1 + \partial_2 u \mathbf{e}_2$  and, for any  $\mathbf{A} \in \mathbb{R}^3 \times \mathbb{R}^3$ , let  $(\mathbf{A})^s = (\mathbf{A} + \mathbf{A}^T)/2$ . In homogeneous *isotropic* linear elasticity theory, the infinitesimal strain is  $\mathbf{E} = (\mathbf{e}_3 \otimes \nabla u)^s$  and the stress reads  $\mathbf{T} = 2\mu(\mathbf{e}_3 \otimes \nabla u)^s$ , having denoted by  $\mu$  the shear elastic modulus. For this case, the elastic strain energy density takes the form  $w = \frac{1}{2}\mu|\nabla u|^2$ .

For what the boundary conditions is concerned, we assume the partition  $\partial\Omega = \overline{\partial\Omega^{\mathcal{N}}} \cup \overline{\partial\Omega^{\mathcal{D}}}$ ,  $\partial\Omega^{\mathcal{N}} \cap \partial\Omega^{\mathcal{D}} = \emptyset$ . Then, we assume that  $\partial\Omega^{\mathcal{N}} \times (-h/2, h/2)$  is traction free, whereas on the remaining part of the lateral surface  $\partial\Omega^{\mathcal{D}} \times (-h/2, h/2)$  the displacement  $\mathbf{u} = \bar{\mathbf{u}} \equiv \bar{u}\mathbf{e}_3$  is prescribed, with  $\bar{u} : \partial\Omega^{\mathcal{D}} \rightarrow \mathbb{R}$ . On the bases  $x_3 = \pm h/2$ , in the most general case we imagine a constraint similar to an elastic foundation *à la* Winkler, i.e., the body is connected by a layer of springs to a support that can rigidly deform. In particular, we assume that the displacement of the support is  $\mathbf{u}(\mathbf{x}, \pm h/2) = \hat{\mathbf{u}} \equiv g(\mathbf{x})\mathbf{e}_3$ , with  $g \in L^\infty(\Omega, \mathbb{R})$ , so that  $\kappa[g(\mathbf{x}) - u(\mathbf{x})]\mathbf{e}_3$  represents the resultant of the force per unit area acting at  $(\mathbf{x}, h/2)$  and  $(\mathbf{x}, -h/2)$ , being  $\kappa$  associated with the corresponding Winkler's constants. Of course, the case  $\kappa = 0$  coincides with that of traction-free bases.

Assume that  $u \in SBV(\Omega)$  and let  $S_u \subset \Omega$  denote the singular set of  $u$ . Then  $K_u := S_u \times (-h/2, h/2)$  is the surface of possible location of plastic slips. Because of the assumed independence of the displacement field and boundary conditions upon the coordinate  $x_3$  integration on  $\mathcal{B}$  can be reduced to an integration on  $\Omega$  and the total energy of the body is  $\Pi(u)h$ , where

$$\Pi(u) := \frac{1}{2}\mu \int_{\Omega \setminus S_u} |\nabla u|^2 d\mathbf{x} + \frac{1}{2}\bar{\kappa} \int_{\Omega \setminus S_u} (g - u)^2 d\mathbf{x} + \gamma \mathcal{H}^1(S_u) + \sigma_0 \int_{S_u} |u^+ - u^-| d\mathcal{H}^1, \quad (3.1)$$

where  $\bar{\kappa} = \kappa/h$  while  $\gamma$  and  $\sigma_0$  are material constants whose significance will be explained soon.

Then we would like to consider the variational problem  $\min_{u \in \mathcal{A}} \Pi(u)$  where the class  $\mathcal{A}$  of admissible functions is defined as

$$\mathcal{A} = \{u \in SBV(\Omega, \mathbb{R}); u = \bar{u} \text{ on } \partial\Omega^{\mathcal{D}}\}, \quad (3.2)$$

where with  $u = \bar{u}$  on  $\partial\Omega^{\mathcal{D}}$  we intend that the trace of  $u$  on  $\partial\Omega^{\mathcal{D}}$  is equal to  $\bar{u}$ . Unfortunately this problem is not well posed since it may happen for a minimizing sequence that the limit does not belong to the class  $\mathcal{A}$ , in the sense that the Dirichlet boundary datum may possibly not be preserved at the limit because of the properties of SBV functions. In other words, no energy would be paid for a displacement-discontinuity occurring right at the Dirichlet boundary. In order to by-pass this difficulty there can be two strategies. One of these, pursued e.g. in [28], is to artificially enlarge the domain  $\Omega$  to, say,  $\Omega^{\mathcal{D}}$ , with  $\Omega^{\mathcal{D}} \cap \partial\Omega = \partial\Omega^{\mathcal{D}}$  and impose, as a boundary datum, that  $u = \bar{u}$  on  $\Omega^{\mathcal{D}} \setminus \bar{\Omega}$ . The second possibility, here preferred, is to relax the problem into the following weaker formulation

$$\min_{u \in SBV(\Omega, \mathbb{R})} \left( \Pi(u) + \gamma \mathcal{H}^1(\{\mathbf{x} \in \partial\Omega^{\mathcal{D}} : u(\mathbf{x}) \neq \bar{u}\}) + \sigma_0 \int_{\partial\Omega^{\mathcal{D}}} |u - \bar{u}| d\mathcal{H}^1 \right), \quad (3.3)$$

which, in physical terms, corresponds to explicitly consider the energy consumption necessary to have a displacement discontinuity at the Dirichlet boundary. The corresponding problem is now well-posed and, by standard semi-continuity and compactness results, it admits a minimizer  $u \in SBV(\Omega, \mathbb{R})$  which fulfills the requirements of the model. However, for the sake of simplicity, here we will not make this distinction explicit but we will declare, unless the distinction is specifically needed, that minimizers are to be sought in the class  $\mathcal{A}$  of (3.2), assuming that such a notation implies the introduction of the relaxed minimization problem (3.3).

As anticipated in Sec. 2, each term of the functional (3.1) has a precise physical meaning. The first integral represents the *elastic strain energy* stored in the sound, elastically bent, material portions. The second integral is not essential, but has been introduced to accentuate the analogies with the the Mumford-Shah functional in problems of image-segmentation, considered in [3]; here, such term denotes the energy of the elastic spring layers *à la* Winkler, connecting the bases of the body to the rigidly-deformed support.

The third and fourth integrals are associated, respectively, with the *surface unpinning energy* to break free the glide surfaces and with the *surface plastic energy*, i.e. the work per unit area that must be expended in order to produce plastic slip, supposed to occur at constant yielding shear stress  $\sigma_0$  (perfect plasticity). In other words, in order break the anchoring link of a potential slip surface, a certain amount of energy has to be consumed: this effect is interpreted by the parameter  $\gamma$  of (3.1), having the dimensions of an energy per unit area. On the other hand, the quantity  $\sigma_0$  of (3.1) is the force per unit area that is necessary to produce gliding of the contact surfaces in the overstrained condition.

Of course, the functional of (3.1) differs from that proposed in [28] essentially because of the presence of the last integral term. These analogies confirm the strict correlation between the models of fracture and yielding [23]. Finally, it should be mentioned that the model here proposed neglects the important phenomenon of strain-hardening.

### 3.3 The regularized approximating functional

The solution of the problem (3.3) is difficult because, in general, the location of the set  $S_u$  is unknown, hence the term “free-discontinuity problems” with which problems of this kind are usually referred to. Following the same strategy pursued for the weak formulation of the Mumford-Shah functional in problems of image-segmentation [3], we propose to approximate the functional  $\Pi(u)$  of (3.1) with the elliptic two-field functional  $\Pi_\varepsilon(u, s)$  defined as

$$\begin{aligned} \Pi_\varepsilon(u, s) &:= \frac{1}{2}\mu \int_{\Omega} (s^2 + o_\varepsilon) |\nabla u|^2 d\mathbf{x} + \frac{1}{2}\bar{\kappa} \int_{\Omega} (g - u)^2 d\mathbf{x} \\ &+ \gamma \int_{\Omega} \left( \varepsilon |\nabla s|^2 + \frac{(1-s)^2}{4\varepsilon} \right) d\mathbf{x} + \sigma_0 \int_{\Omega} (1-s)^2 |\nabla u| d\mathbf{x}, \end{aligned} \quad (3.4)$$

where here  $o_\varepsilon$  is an infinitesimal faster than  $\varepsilon$ . The approximating variational problem then becomes

$$\min_{(u,s) \in \hat{\mathcal{A}}} \Pi_\varepsilon(u, s), \quad (3.5)$$

where the class  $\hat{\mathcal{A}}$  of admissible functions now becomes

$$\hat{\mathcal{A}} = \{(u, s) \in W^{1,2}(\Omega, \mathbb{R}) \times W^{1,2}(\Omega, \mathbb{R}); u = \bar{u} \text{ on } \partial\Omega^{\mathcal{D}} \text{ and } s = 1 \text{ on } \partial\Omega^{\mathcal{D}}\}. \quad (3.6)$$

The compactness result in [3] guarantees the existence of a minimizing pair in  $W^{1,2}(\Omega, \mathbb{R}) \times W^{1,2}(\Omega, \mathbb{R})$ . In particular, by the Sobolev imbedding, those solutions are automatically  $C^{0,1/2}$  in dimension 1, but the discussion of the regularity in higher dimension is more complicated and goes beyond the scope of this paper.

The aforementioned approximation is in the sense of a type of variational convergence referred to as  $\Gamma$ -convergence which, roughly speaking, describes in mathematical terms how a sequence of functionals depending upon a parameter converges to a desired functional as that parameter tends to zero. Remarkably,  $\Gamma$ -convergence implies convergence of both minima and minimizers. Here the aforementioned parameter is  $\varepsilon$  and we will prove in the next Section that as  $\varepsilon \rightarrow 0$  the functional of (3.4)  $\Gamma$ -converges to the functional of (3.1).

The proposed approximation is *almost* identical to that of [11]. The main difference consists in the last integral on the r.h.s. of (3.1), whose counterpart is the last integral in (3.4) and, indeed, our main result here consists in proving the convergence of the latter to the former one. Another difference with the treatment presented in [11] consists in the boundary conditions for  $s$  in (3.6). Instead of introducing, as in [11], an enlarged logical domain to recover a correct value for the surface energy of fractures developing at the boundary, for the reasons already discussed at length in [37] and confirmed in [4], here we assume the condition  $s = 1$  at the constrained borders that bypasses this problem because it forbids the development of fractures exactly at the boundary, although they are free to appear at a small distance (of the order of  $\varepsilon$ ). This effect may well interpret the confining effects offered in a real experimental set-up by fractional contact or gluing of the supports, and indeed is in agreement with the formulation of (3.3).

Last but not least, it should be mentioned that although the regularized reformulation is viewed by many as a numerical method only akin to bypass a difficult free-discontinuity problem<sup>2</sup>, others insist that the formulation carries additional physical information. This means that the regularized problem (3.5) is not just a useful approximation of (3.3), but an independent model *per se*. As discussed in very keen but perhaps forgotten contributions<sup>3</sup>, the phenomenon of plastic slip is not atomically sharp but distributed on layers of small but not negligible thickness [39]. This is due to the fact that yielding is not a local phenomenon but instead it is influenced by the stress distribution in the neighboring parts. We will show later on that regularized functional (3.4) views this kinematics as a physical representation of a smeared slip surface, occurring in a band whose thickness is of the same order of the parameter  $\varepsilon$ . In more precise terms, the functional (3.1) considers a surface source of dissipation, whereas the formulation (3.4) prescribes a bulk source of dissipation in layers approximately  $\varepsilon$ -thick.

<sup>2</sup>The interest is not limited to fracture mechanics, but similar regularizations can be found in front capturing methods in gas dynamics (level set method) or phase field methods in the theory of defects.

<sup>3</sup>To this respect, we should mention the almost unknown work by Nakanishi and [40] in particular.

Indeed, the regularized functional embraces the material parameter  $\varepsilon$  that is lost in the limit free-discontinuity functional corresponding to  $\varepsilon \rightarrow 0$ . Thus,  $\varepsilon$  disappears in the functional (3.1) but this represents an information about the material microstructure because it plays the physical role of the material *intrinsic length-scale*, that characterizes the width of the slip bands. In conclusion, according to this interpretation, the regularized functional is *the model*, while its parent  $\Gamma$ -limit (the free-discontinuity problem) is the *approximation*. However, in this paper we do not pursue this quite subtle distinction and we limit ourselves to discuss the main characteristics of the two models and their relationship *via*  $\Gamma$ -convergence.

### 3.4 Irreversibility of plastic slip

As stated, the variational problems presented in the previous sections would presuppose that all deformations are perfectly reversible. On the other hand it is well-known that this is not the case in plasticity, where the issue of unloading, in particular, represents one of the major difficulties. At the moment, it is not so clear how to represent all loading scenarios, but the formulations of Section 3.2 and 3.3 are certainly able to represent a loading history where the plastic slip is a monotone increasing function.

More precisely, following [10], we assume a loading history where, in the classes of admissible functions  $\mathcal{A}$  of<sup>4</sup> (3.2) and  $\hat{\mathcal{A}}$  of (3.6),  $\bar{u}$  is a function of the parameter  $t$ , representative of the time, i.e.,  $\bar{u} = \bar{u}(t)$ . We will emphasize this dependence indicating with  $\mathcal{A}(t)$  and  $\hat{\mathcal{A}}(t)$  the classes  $\mathcal{A}$  and  $\hat{\mathcal{A}}$  where such substitution has been made. In general, in the *evolution problem* we assume that the time interval  $[0, T]$  of the loading history is discretized into steps  $0 \leq t_i \leq t_p \equiv T$ ,  $1 \leq i \leq p$ , with  $p \gg 1$  so that each time-step is sufficiently small.

Referring first to problem (3.1), (3.3) and (3.2), let  $\bar{u}_i = \bar{u}(t_i)$ ,  $\mathcal{A}_i = \mathcal{A}(t_i)$  and let  $u_i$  represent the displacement field solution of the evolution problem at the time  $t = t_i$ . Denoting with  $S_{u_i}$  the set of jump points of  $u_i$ , we define

$$\Upsilon_i = \bigcup_{0 \leq j \leq i} S_{u_j} . \quad (3.7)$$

Then, the displacement field  $u_{i+1}$  at time  $t = t_{i+1}$  is the solution of the variational problem

$$\min_{u \in \mathcal{K}_{i+1}} \Pi^i(u) , \quad (3.8)$$

where

$$\mathcal{K}_{i+1} = \{u \in \mathcal{A}_{i+1} : J_u \supseteq \Upsilon_i\} , \quad (3.9)$$

and

---

<sup>4</sup>Here, to be rigorous, we should refer to the relaxed minimization problem (3.3), but for the sake of simplicity we will drop this distinction that does not produce substantial differences.

$$\begin{aligned}
 \Pi^i(u) &:= \frac{1}{2}\mu \int_{\Omega \setminus S_u} |\nabla u|^2 d\mathbf{x} + \gamma \mathcal{H}^1(S_u) + \frac{1}{2}\bar{\kappa} \int_{\Omega \setminus J_u} (g - u)^2 d\mathbf{x} \\
 &+ \sigma_0 \int_{S_u} \{ |(u^+ - u^-) - (u_i^+ - u_i^-)| + |(u_i^+ - u_i^-)| \} d\mathcal{H}^1. \quad (3.10)
 \end{aligned}$$

In this expression, the significance of the last integral is to represent that any variation of the plastic slip during the loading history must be associated with energy consumption, even when the slip goes backwards. This is because, whatever the direction of the slip, the shear stress always opposes to the motion, thus representing some sort of frictional-like constraint for the slip movement. It is worth mentioning that the last term  $|(u_i^+ - u_i^-)|$  in (3.10) is constant for each step  $i$ , thus does not affect the minimization problem, but we keep it in the expression of  $\Pi^i(u)$  in order to preserve the physical value of the energy.

Of course, if during the loading history the plastic slip is a monotone function, i.e., if  $|u_{i+1}^+ - u_{i+1}^-| \geq |u_i^+ - u_i^-|$  for any  $1 \leq i \leq p$ , then the functional  $\Pi^i(u)$  of (3.10) is identical to  $\Pi(u)$  of (3.1), the set  $\Upsilon_{i+1} \supseteq \Upsilon_i$ , and the evolution problem reduces to the minimization problem of Section 3.2.

Passing now to the regularized problem (3.4), (3.5) and (3.6) let, as before,  $\bar{u}_i = \bar{u}(t_i)$ ,  $\hat{A}_i = \hat{A}(t_i)$  and assume that  $(u_i, s_i)$  is the field corresponding to the evolution problem at  $t = t_i$ . Then the field  $(u_{i+1}, s_{i+1})$  at  $t = t_{i+1}$  corresponds to the solution of the minimization problem

$$\min_{(u,s) \in \hat{\mathcal{K}}_{i+1}} \Pi_\varepsilon^i(u, s), \quad (3.11)$$

with

$$\hat{\mathcal{K}}_{i+1} = \{(u, s) \in W^{1,2}(\Omega)^2 ; s \leq s_i\}, \quad (3.12)$$

and

$$\begin{aligned}
 \Pi_\varepsilon^i(u, s) &:= \frac{1}{2}\mu \int_{\Omega} (s^2 + o_\varepsilon) |\nabla u|^2 d\mathbf{x} + \frac{1}{2}\bar{\kappa} \int_{\Omega} (g - u)^2 d\mathbf{x} \\
 &+ \gamma \int_{\Omega} \left[ \varepsilon |\nabla s|^2 + \frac{(1-s)^2}{4\varepsilon} \right] d\mathbf{x} \\
 &+ \sigma_y \int_{\Omega} (1-s)^2 (|\nabla u - \nabla u_i| + |\nabla u_i|) d\mathbf{x}. \quad (3.13)
 \end{aligned}$$

The last integral in this expression represents the counterpart of the last integral in (3.10), and again represents, in a smeared view, that a certain amount of work must always be spent to produce plastic deformation.

Of course, as the reference time step tends to zero, the solution of the series of minimization problems define a more and more accurate description of the evolution process. However, a precise mathematical characterization of such a limit is not available at the

moment and we refer to the pioneering works [10, 11, 20, 13, 28] for a similar evolution problem for the case of brittle fracture.

## 4 Regularized formulation and the approximation result

### 4.1 Review on Gamma-convergence

Gamma-convergence of energy functionals is commonly understood as the natural notion of convergence, in a variational context, ensuring that limit points of minimizers are minimizers. For an introductory (but complete) survey on Gamma-convergence theory one could see the book by Dal Maso [19]. The definition that will be used here is the following.

**Definition 1** ( $\Gamma$ -convergence). *Given a Hilbert space  $H$  and a sequence of functionals  $F_n : H \rightarrow \mathbb{R} \cup \{+\infty\}$ , we say that  $F_n$   $\Gamma$ -converges to  $F$  if for every  $u \in H$  the two following properties hold :*

- i) for every sequence  $u_n \rightarrow u$  one has  $F(u) \leq \liminf_{n \rightarrow +\infty} F_n(u_n)$ ;*
- ii) there exists  $u_n \rightarrow u$  such that  $F(u) \geq \limsup_{n \rightarrow +\infty} F_n(u_n)$ .*

**Remark 1.** The convergence  $u_n \rightarrow u$  means for the topology of  $H$ .

The interesting fact about Gamma-convergence is that if  $F_n$  Gamma-converge to  $F$  and if  $u_n$  are asymptotically minimizing, i.e.,

$$\lim_{n \rightarrow +\infty} \left( F_n(u_n) - \inf_H F_n \right) = 0,$$

then any limit point  $u$  of  $u_n$  is a minimizer of  $F$ .

### 4.2 The approximation result

For simplicity we will assume in this paragraph that all the physical constants are equal to 1 which, certainly, is not a loss of generality for what the  $\Gamma$ -convergence result is concerned. As a consequence for  $\Omega \subset \mathbb{R}^N$ ,  $g \in L^\infty(\Omega)$ ,  $u, s \in H^1(\Omega)$  and  $\varepsilon > 0$  the functional  $\Pi_\varepsilon(u, s)$  introduced in (3.4) becomes

$$\Pi_\varepsilon(u, s) := \int_\Omega (u-g)^2 + \int_\Omega (s^2 + o_\varepsilon) |\nabla u|^2 dt + \left( \int_\Omega \varepsilon |\nabla s|^2 + \frac{(1-s)^2}{4\varepsilon} dt \right) + \left( \int_\Omega (1-s)^2 |\nabla u| \right),$$

where  $o_\varepsilon$  is still an infinitesimal faster than  $\varepsilon$ . Next, for  $u \in SBV(\Omega)$  we also consider, as before,

$$\Pi(u) := \int_\Omega (u-g)^2 + \int_\Omega |\nabla u|^2 + \int_{S_u} (1 + |u^+ - u^-|) d\mathcal{H}^{N-1}.$$

Now we define a family of functionals on  $H := [L^2(\Omega)]^2$ .

$$\mathcal{F}_\varepsilon(u, s) := \begin{cases} \Pi_\varepsilon(u, s) & \text{if } u, s \in H^1(\Omega) \text{ and } 0 \leq s \leq 1 \\ +\infty & \text{otherwise} \end{cases}$$

and also the limiting functional

$$\mathcal{F}(u, s) := \begin{cases} \Pi(u) & \text{if } u \in SBV(\Omega) \text{ and } s = 1 \\ +\infty & \text{otherwise.} \end{cases}$$

As in [3] we will assume  $\Omega$  to be a domain satisfying the following reflection property called  $(R)$ : there exist a neighborhood  $U$  of  $\partial\Omega$  and a bi-Lipschitz mapping  $\varpi : U \cap \Omega \rightarrow U \setminus \bar{\Omega}$  such that

$$\lim_{y \rightarrow x} \varpi(y) = x \quad \forall x \in \partial\Omega.$$

Any sufficiently smooth domain (e.g. Lipschitz) has the property  $(R)$ . Our main result is the following.

**Theorem 4.1.** *Under the above notations and assumptions,  $\mathcal{F}_\varepsilon$   $\Gamma$ -converge to  $\mathcal{F}$  for the  $L^2$  topology.*

As usual in Gamma-convergence results, we will separate the proof in two parts.

### 4.3 Proof of the lower inequality

**Proposition 1.** *For every pair of functions  $(u, s) \in SBV(\Omega)^2$  and for every  $(u_\varepsilon, s_\varepsilon) \in H^1(\Omega) \times H^1(\Omega)$  converging to  $(u, s)$  in  $L^2(\Omega)$  we have that*

$$\mathcal{F}(u, s) \leq \liminf_{\varepsilon \rightarrow 0} \mathcal{F}_\varepsilon(u_\varepsilon, s_\varepsilon). \quad (4.1)$$

*Proof.* Just for notational simplicity we will keep the continuous parameter  $\varepsilon$  also when, during the proof, some subsequences from  $(u_\varepsilon, s_\varepsilon)$  have to be extracted. It is enough to prove (4.1) for a sequence  $(u_\varepsilon, s_\varepsilon)$  that achieves the  $\Gamma$ -liminf, i.e.

$$\lim_{\varepsilon \rightarrow 0} \mathcal{F}_\varepsilon(u_\varepsilon, s_\varepsilon) = \inf \left\{ \liminf_{\varepsilon \rightarrow 0} \mathcal{F}_\varepsilon(v_\varepsilon, s_\varepsilon); (v_\varepsilon, s_\varepsilon) \rightarrow (u, s) \text{ in } L^2 \right\}.$$

In particular for this sequence  $(u_\varepsilon, s_\varepsilon)$ , since  $\mathcal{F}_\varepsilon(u_\varepsilon, s_\varepsilon)$  is uniformly bounded, we deduce that  $s_\varepsilon$  converges to 1 in  $L^2$  which implies  $s = 1$  a.e. and  $\mathcal{F}(u, s) = \Pi(u)$ . Let us split in two parts the functional and write  $\Pi_\varepsilon = AT_\varepsilon + G$  where, for  $U \subset \Omega$ ,

$$AT_\varepsilon(u, s, U) := \int_U (u - g)^2 + \int_U (s^2 + o_\varepsilon) |\nabla u|^2 dx + \int_U \varepsilon |\nabla s|^2 + \frac{(1-s)^2}{4\varepsilon} dx,$$

and

$$G(u, s, U) := \int_U (1-s)^2 |\nabla u|^2 dx.$$

Without loss of generality we may assume that  $|s_\varepsilon \nabla u_\varepsilon|$  weakly converge in  $L^2(\Omega)$  to some function  $f$  and that the sequence of measures

$$\sigma_\varepsilon := \left( (u_\varepsilon - g)^2 + (s_\varepsilon^2 + o_\varepsilon) |\nabla u_\varepsilon|^2 + \varepsilon |\nabla s_\varepsilon|^2 + \frac{(1 - s_\varepsilon)^2}{4\varepsilon} + (1 - s_\varepsilon)^2 |\nabla u_\varepsilon| \right) \mathcal{L}^N$$

weakly converges to a measure  $\sigma$ , whose total mass in  $\Omega$  is less than  $\lim_{\varepsilon \rightarrow 0} \Pi_\varepsilon(u_\varepsilon, s_\varepsilon)$ . Therefore, to prove the Proposition it is enough to show that

$$\sigma(\Omega) \geq \Pi(u).$$

By the  $\Gamma$ -convergence result of [3], and more precisely by the lower inequality in [3], we infer that for any open set  $U \subset \Omega$ ,

$$\liminf_{\varepsilon \rightarrow 0} \Pi_\varepsilon(u_\varepsilon, s_\varepsilon, U) \geq MS(u, U),$$

where  $MS$  is the classical Mumford-Shah functional

$$MS(u, U) := \int_U (u - g)^2 + \int_{\Omega \setminus S_u} |\nabla u|^2 dx + \mathcal{H}^{N-1}(S_u \cap U).$$

In particular this yields

$$\sigma(\bar{U}) \geq MS(u, U)$$

and, by inner approximation of  $A$  open with  $U \Subset A$ , we then get  $\sigma(A) \geq MS(u, A)$  for all  $A$  open. Eventually, by outer approximation with open sets, we get

$$\sigma(B) \geq MS(u, B) \quad \text{for all Borel sets } B. \quad (4.2)$$

On the other hand, if we add and subtract  $|\nabla u_\varepsilon|$ , for any open set  $U \subset \Omega$  we get

$$\begin{aligned} \Pi_\varepsilon(u_\varepsilon, s_\varepsilon, U) &= AT_\varepsilon(u_\varepsilon, s_\varepsilon, U) + \int_U |\nabla u_\varepsilon| dx + \int_U (s_\varepsilon^2 - 2s_\varepsilon) |\nabla u_\varepsilon| dx \\ &\geq AT_\varepsilon(u_\varepsilon, s_\varepsilon, U) + \int_U |\nabla u_\varepsilon| dx - 2 \int_U |s_\varepsilon \nabla u_\varepsilon| dx \end{aligned} \quad (4.3)$$

thus passing to the  $\liminf$ , since  $\int_U |s_\varepsilon \nabla u_\varepsilon| dx$  converges to  $\int_U f dx$  and by the lower semi-continuity property of the total variation with respect to the  $L^2$  topology it comes

$$\sigma(\bar{U}) \geq MS(u, U) + |Du|(U) - 2 \int_U f dx.$$

Again, by the same approximations leading to (4.2), we get

$$\sigma(B) \geq MS(u, B) + |Du|(B) - 2 \int_B f dx. \quad (4.4)$$

for all Borel sets  $B$ . Gathering together (4.2) with  $B = \Omega \setminus S_u$  and (4.4) with  $B = S_u$  we obtain that

$$\begin{aligned} \sigma(\Omega) &= \sigma(\Omega \setminus S_u) + \sigma(S_u) \\ &\geq \int_{\Omega} (u - g)^2 + \int_{\Omega \setminus S_u} |\nabla u|^2 + \int_{S_u} 1 + |u^+ - u^-| d\mathcal{H}^{N-1} \\ &= \Pi(u) \end{aligned}$$

which ends the proof.  $\square$

#### 4.4 Proof of the upper inequality

To prove the upper inequality we will need some standard convolution techniques. Let  $\varphi$  be a smooth function taking values in  $[0, 1]$  satisfying  $\text{supp}(\varphi) \subset B(0, 1)$  and  $\int \varphi = 1$ . Then for any  $t > 0$  we define the family of mollifiers  $\varphi_t(x) := t^{-N} \varphi(x/t)$ . If  $\mu$  is any probability measure on  $\mathbb{R}^N$  with compact support we define the convolution with  $\varphi_t$  by  $\mu * \varphi_t(x) := \int_{\mathbb{R}^N} \varphi_t(x - y) d\mu(y)$ . The following Lemma is very classical and a proof can be found for instance in [2, Th. 2.2.].

**Lemma 1.** *Let  $\mu$  be a probability measure on  $\mathbb{R}^N$  with compact support. Then  $\mu * \varphi_t \in L^1(\mathbb{R}^N)$  and the measures  $(\mu * \varphi_t) \mathcal{L}^N$  locally weakly- $\star$  converge in  $\mathbb{R}^N$  to  $\mu$  as  $t \rightarrow 0$ . Moreover the estimate*

$$\int_{\mathbb{R}^N} |\mu * \varphi_t|(x) dx \leq |\mu|(\mathbb{R}^N)$$

holds.

**Remark 2.** It follows from an easy computation (see [2, 3.2.(c)]) that when  $u \in BV(\mathbb{R}^N)$  then  $\nabla(u * \varphi_\varepsilon) = (Du) * \varphi_\varepsilon$ , where  $Du$  is the distributional derivative of  $u$ .

We are now ready to prove the second half of our  $\Gamma$ -convergence result.

**Proposition 2.** *For every  $(u, s) \in SBV(\Omega) \times L^\infty(\Omega)$  there exist  $(u_\varepsilon, s_\varepsilon) \in C^1(\Omega) \times C^1(\Omega)$  converging to  $(u, s)$  in  $L^2(\Omega)$  such that*

$$\limsup_{\varepsilon \rightarrow 0} \mathcal{F}_\varepsilon(u_\varepsilon, s_\varepsilon) \leq \mathcal{F}(u, s). \quad (4.5)$$

*Proof.* We may assume without loss of generality that  $s = 1$  (otherwise the right-hand side of (4.5) is  $+\infty$  and there is nothing to prove). Since the functionals  $\Pi_\varepsilon$  are strongly continuous in the  $H^1(\Omega)$  space and since  $C^1(\Omega)$  is dense, it will be enough to find  $u_\varepsilon$  and  $s_\varepsilon$  in  $H^1(\Omega)$ . We may also assume that  $S_u$  is closed and  $u$  is bounded. The reduction to this case will be explained at the end of the proof.

The beginning of the proof has no difference with the argument of [3]. Let  $S_u$  be the singular set of  $u$  and for any  $t$  we will denote

$$(S_u)_t := \{x \in \mathbb{R}^N; \text{dist}(x, S_u) \leq t\} \subset \mathbb{R}^N.$$

As in [3] we first assume that

$$\lim_{\rho \rightarrow 0} \frac{\mathcal{L}^N(\Omega \cap (S_u)_\rho)}{2\rho} = \mathcal{H}^{N-1}(S_u). \quad (4.6)$$

Then, for some suitable infinitesimals  $a_\varepsilon$ ,  $b_\varepsilon$  and  $\eta_\varepsilon$  we take the same function  $s_\varepsilon$  as in the proof of Theorem 3.1. in [3], namely

$$s_\varepsilon = \begin{cases} 0 & \text{on } (S_u)_{b_\varepsilon} \\ 1 - \eta_\varepsilon & \text{on } \Omega \setminus (S_u)_{a_\varepsilon + b_\varepsilon} \\ 1 - \exp\left(\frac{b_\varepsilon - \text{dist}(x, S_u)}{2\varepsilon}\right) & \text{on } (S_u)_{a_\varepsilon + b_\varepsilon} \setminus (S_u)_{b_\varepsilon} \end{cases}$$

From [3] page 116-117, we know that (and the proof is omitted here) by choosing  $b_\varepsilon$  between  $o_\varepsilon$  and  $\varepsilon$  (for instance  $b_\varepsilon = \sqrt{o_\varepsilon \varepsilon}$ ), taking  $\eta_\varepsilon = \varepsilon$ ,  $a_\varepsilon = -2\varepsilon \ln(\eta_\varepsilon)$ , that we know to be infinitesimal, and under the assumption (4.6), then

$$\limsup_{\varepsilon \rightarrow 0} \left( \int_\Omega \varepsilon |\nabla s_\varepsilon|^2 + \frac{(1 - s_\varepsilon)^2}{4\varepsilon} \right) \leq \mathcal{H}^{N-1}(S_u).$$

Now comes the differences with [3]. In order to construct  $u_\varepsilon$  we first need to define a SBV extension for  $u$  outside  $\Omega$  in the neighborhood  $U$ , i.e. the one given by the regularity assumption (R). We denote  $\tilde{u}$  this extension that we define by

$$\tilde{u}(x) = \begin{cases} u(\varpi^{-1}(x)) & \text{for } x \in U \setminus \bar{\Omega} \\ u(x) & \text{for } x \in \Omega \end{cases}$$

By this way  $\tilde{u} \in SBV(\Omega \cup U)$  (see for instance [3, 51, 50]) and

$$\mathcal{H}^{N-1}(S_{\tilde{u}} \cap \partial\Omega) = 0.$$

In the sequel the distinction between  $S_u$ , that we always consider as a subset of  $\Omega$ , and  $S_{\tilde{u}} \subset \Omega \cup U$  will be important. Next we take a smooth cutoff function  $\psi_\varepsilon$  equal to 1 on  $(S_u)_{b_\varepsilon/2}$ , equal to 0 on  $\mathbb{R}^N \setminus (S_u)_{\frac{3}{4}b_\varepsilon}$ , and such that

$$|\nabla \psi_\varepsilon| \leq \frac{C}{b_\varepsilon} \quad \text{and} \quad |\nabla^2 \psi_\varepsilon| \leq \frac{C}{b_\varepsilon^2}. \quad (4.7)$$

Such a function  $\psi_\varepsilon$  can be constructed for instance by convolution of the characteristic function  $\mathbf{1}_{(S_u)_{3b_\varepsilon/8}}$  with the standard mollifier obtained by a suitable rescaling of  $\mathbf{1}_{|x|<1} \exp(-\frac{1}{1-|x|^2})$ . Then we define

$$u_\varepsilon = (1 - \psi_\varepsilon)\tilde{u} + (\psi_\varepsilon \tilde{u}) * \varphi_{t_\varepsilon}$$

where  $\varphi_{t_\varepsilon}$  is a mollifier and where we choose  $t_\varepsilon = b_\varepsilon^4$ . In particular we assume  $b_\varepsilon$  and  $t_\varepsilon$  to be small enough with respect to the size of  $U$  so that  $u_\varepsilon$  is well defined. Notice that  $u_\varepsilon \in SBV(\Omega \cup U) \cap H^1(\Omega)$ . Notice also that from Lemma 1 we have that  $(\psi_\varepsilon D\tilde{u}) * \varphi_{t_\varepsilon} \in L^1(\mathbb{R}^N)$  and since  $\text{supp}((\psi_\varepsilon D\tilde{u}) * \varphi_{t_\varepsilon}) \subset (S_u)_{b_\varepsilon + t_\varepsilon}$ , we also get from Lemma 1 that

$$\int_{\mathbb{R}^N} |(\psi_\varepsilon D\tilde{u}) * \varphi_{t_\varepsilon}| dx \leq |D\tilde{u}|((S_u)_{b_\varepsilon + t_\varepsilon}). \quad (4.8)$$

We may also assume  $t_\varepsilon$  small enough in such a way that  $\text{supp}((\psi_\varepsilon D\tilde{u}) * \varphi_{t_\varepsilon}) \subset (S_u)_{b_\varepsilon}$  thus  $u_\varepsilon = u$  in  $\Omega \setminus (S_u)_{b_\varepsilon}$  because by definition,  $\psi_\varepsilon$  is compactly supported in  $(S_u)_{b_\varepsilon}$ .

By our choice of  $s_\varepsilon$  and  $u_\varepsilon$  we easily get

$$\lim_{\varepsilon \rightarrow 0} \int_{\Omega} |u_\varepsilon - g|^2 = \int_{\Omega} |u - g|^2.$$

Therefore, it remains to prove the following two assertions:

$$i) \quad \limsup_{\varepsilon \rightarrow 0} \int_{\Omega} (s_\varepsilon^2 + o_\varepsilon) |\nabla u_\varepsilon|^2 \leq \int_{\Omega \setminus S_u} |\nabla u|^2, \quad (4.9)$$

$$ii) \quad \limsup_{\varepsilon \rightarrow 0} \int_{\Omega} (1 - s_\varepsilon)^2 |\nabla u_\varepsilon| \leq \int_{S_u} |u^+ - u^-| d\mathcal{H}^{N-1}. \quad (4.10)$$

We begin with (4.9). Since

$$\mathbf{1}_\Omega s_\varepsilon^2 |\nabla u_\varepsilon|^2 \leq \mathbf{1}_{\Omega \setminus (S_u)_{b_\varepsilon}} |\nabla u|^2,$$

we obtain that  $\limsup \int_{\Omega} s_\varepsilon^2 |\nabla u_\varepsilon|^2 dx \leq \int_{\Omega \setminus S_u} |\nabla u|^2$ . Now owing to Remark 2, a direct computation shows that

$$\nabla u_\varepsilon = (1 - \psi_\varepsilon) \nabla \tilde{u} + ((\tilde{u} \nabla \psi_\varepsilon) * \varphi_{t_\varepsilon} - \tilde{u} \nabla \psi_\varepsilon) + (\psi_\varepsilon D\tilde{u}) * \varphi_{t_\varepsilon}, \quad (4.11)$$

and we claim that each term multiplied by  $\sqrt{o_\varepsilon}$  tends to 0 in  $L^2$ , which is enough to conclude the proof of (4.9). The control of the first term is immediate, namely

$$o_\varepsilon \int_{\Omega} (1 - \psi_\varepsilon) |\nabla \tilde{u}|^2 \xrightarrow{\varepsilon \rightarrow 0} 0.$$

Subsequently since  $\varphi_{t_\varepsilon}$  is a mollifier we have  $\int \varphi_{t_\varepsilon} = 1$  thus by young's inequality we can estimate the last term as

$$\begin{aligned} o_\varepsilon \int_{\Omega} |(\psi_\varepsilon D\tilde{u}) * \varphi_{t_\varepsilon}|^2 &\leq o_\varepsilon \left( \int_{\Omega \setminus S_u} |\nabla \tilde{u}|^2 \right) \left( \int_{\mathbb{R}^N} |\varphi_{t_\varepsilon}| \right)^2 \\ &\leq o_\varepsilon \left( \int_{\Omega \setminus S_u} |\nabla \tilde{u}|^2 \right) \xrightarrow{\varepsilon \rightarrow 0} 0. \end{aligned}$$

Now for the intermediate term, we claim that by our choice of  $t_\varepsilon$  it converges itself to zero in  $L^2$  (without need of multiplying it by  $o_\varepsilon$ ). Indeed, a standard Lemma on BV functions (see e.g. Lemma 3.24 page 133 of [2]) says that

$$\int_{\Omega \cap (S_u)_{b_\varepsilon}} |(\tilde{u} \nabla \psi_\varepsilon) * \varphi_{t_\varepsilon} - \tilde{u} \nabla \psi_\varepsilon| dx \leq t_\varepsilon |Df_\varepsilon|(\Omega_\delta) \quad (4.12)$$

where  $f_\varepsilon := \tilde{u} \nabla \psi_\varepsilon$  and  $\delta > 0$  is very small, but fixed. In particular by assumption (4.7) on  $\psi_\varepsilon$  we have that  $|Df_\varepsilon|(\Omega_\delta) \leq \frac{C}{b_\varepsilon^2}$ , where  $C$  depends in particular on  $L^\infty$  norm of  $u$ , that we assumed for a moment to be bounded, and (4.12) becomes (since  $\tilde{u}$  is  $u$  inside  $\Omega$ )

$$\int_{\Omega \cap (S_u)_{b_\varepsilon}} |(u \nabla \psi_\varepsilon) * \varphi_{t_\varepsilon} - u \nabla \psi_\varepsilon| dx \leq \frac{C t_\varepsilon}{b_\varepsilon^2}. \quad (4.13)$$

Therefore,

$$\begin{aligned} \|(u\nabla\psi_\varepsilon) * \varphi_{t_\varepsilon} - u\nabla\psi_\varepsilon\|_2^2 &\leq \|(u\nabla\psi_\varepsilon) * \varphi_{t_\varepsilon} - u\nabla\psi_\varepsilon\|_\infty \|(u\nabla\psi_\varepsilon) * \varphi_{t_\varepsilon} - u\nabla\psi_\varepsilon\|_1 \\ &\leq \frac{C}{b_\varepsilon} \times \frac{Ct_\varepsilon}{b_\varepsilon^2} \xrightarrow{\varepsilon \rightarrow 0} 0 \end{aligned}$$

because  $t_\varepsilon = b_\varepsilon^4$ , and now (4.9) is proved.

It remains now to prove (4.10). We split  $\int_\Omega (1 - s_\varepsilon)^2 |\nabla u_\varepsilon|$  in three parts, corresponding to the integration on  $(S_u)_{a_\varepsilon+b_\varepsilon} \setminus (S_u)_{b_\varepsilon}$ ,  $(S_u)_{b_\varepsilon}$  and  $\Omega \setminus (S_u)_{a_\varepsilon+b_\varepsilon}$  (all intersected with  $\Omega$ ). Since  $s_\varepsilon = 1 - \eta_\varepsilon$  and  $u_\varepsilon = u$  on  $\Omega \setminus (S_u)_{a_\varepsilon+b_\varepsilon}$  we have that

$$\int_{\Omega \setminus (S_u)_{a_\varepsilon+b_\varepsilon}} (1 - s_\varepsilon)^2 |\nabla u_\varepsilon| = \eta_\varepsilon^2 \int_{\Omega \setminus (S_u)_{a_\varepsilon+b_\varepsilon}} |\nabla u| \longrightarrow 0 \text{ when } \varepsilon \rightarrow 0. \quad (4.14)$$

Next we treat the integral over  $A_\varepsilon := ((S_u)_{a_\varepsilon+b_\varepsilon} \setminus (S_u)_{b_\varepsilon}) \cap \Omega$ . We first use the definition of  $s_\varepsilon$  and  $u_\varepsilon$  on  $A_\varepsilon$  and then Cauchy-Schwartz inequality to get

$$\begin{aligned} \int_{A_\varepsilon} (1 - s_\varepsilon)^2 |\nabla u_\varepsilon| &= \int_{A_\varepsilon} \exp 2 \left( \frac{b_\varepsilon - d(x, S_u)}{2\varepsilon} \right) |\nabla u| \\ &\leq |A_\varepsilon|^{\frac{1}{2}} \left( \int_{\Omega \setminus S_u} |\nabla u|^2 \right)^{\frac{1}{2}} \end{aligned} \quad (4.15)$$

which tends to zero because  $|A_\varepsilon| \rightarrow 0$  (the exponential in (4.15) is less than 1 because  $b_\varepsilon \leq d(x, S_u)$  on  $A_\varepsilon$ ).

Therefore, it remains to consider the integral over  $\Omega \cap (S_u)_{b_\varepsilon}$ , where in particular  $s_\varepsilon = 0$  thus

$$\int_{\Omega \cap (S_u)_{b_\varepsilon}} (1 - s_\varepsilon)^2 |\nabla u_\varepsilon| = \int_{\Omega \cap (S_u)_{b_\varepsilon}} |\nabla u_\varepsilon|. \quad (4.16)$$

Recall that by (4.11),

$$\nabla u_\varepsilon = (1 - \psi_\varepsilon) \nabla \tilde{u} + ((\tilde{u} \nabla \psi_\varepsilon) * \varphi_{t_\varepsilon} - \tilde{u} \nabla \psi_\varepsilon) + (\psi_\varepsilon D \tilde{u}) * \varphi_{t_\varepsilon},$$

and we already have proved in (4.13) that

$$\int_{\Omega \cap (S_u)_{b_\varepsilon}} |(u \nabla \psi_\varepsilon) * \varphi_{t_\varepsilon} - u \nabla \psi_\varepsilon| dx \rightarrow 0 \text{ when } \varepsilon \rightarrow 0. \quad (4.17)$$

In addition since  $|1 - \psi_\varepsilon| \leq 1$  and with support compactly contained outside  $S_u$ , we easily have that

$$\int_{\Omega \cap (S_u)_{b_\varepsilon}} (1 - \psi_\varepsilon) |\nabla \tilde{u}| \leq \int_{\Omega \cap (S_u)_{b_\varepsilon} \setminus S_u} |\nabla u| \rightarrow 0 \text{ when } \varepsilon \rightarrow 0. \quad (4.18)$$

Subsequently, putting together (4.17), (4.18), and then using inequality (4.8) we obtain

$$\int_{\Omega \cap (S_u)_{b_\varepsilon}} |\nabla u_\varepsilon| \leq o(1) + \int_{\Omega \cap (S_u)_{b_\varepsilon}} |(\psi_\varepsilon D\tilde{u}) * \varphi_{t_\varepsilon}| \leq o(1) + |D\tilde{u}|((S_u)_{b_\varepsilon + t_\varepsilon}).$$

Finally passing to the limsup and using that  $\mathcal{H}^{N-1}(S_{\tilde{u}} \cap \bar{\Omega} \setminus S_u) = 0$  we get

$$\limsup_{\varepsilon \rightarrow 0} \int_{\Omega \cap (S_u)_{b_\varepsilon}} |\nabla u_\varepsilon| \leq |D\tilde{u}|(S_{\tilde{u}} \cap \bar{\Omega}) = \int_{S_u} |u^+ - u^-| d\mathcal{H}^{N-1}$$

which ends the proof of the proposition when the assumption (4.6) holds.

Now to get rid of (4.6) and prove the proposition in full generality, since the argument is quite standard (see [3, 27]) we will only sketch the ideas of proof. Firstly, up to use a truncature and a diagonal argument we can assume that  $u$  is bounded. Then we observe that if  $u \in SBV(\Omega) \cap L^\infty(\Omega)$  is such that  $S_u$  is essentially closed (i.e.  $\mathcal{H}^{N-1}(\bar{S}_u \setminus S_u) = 0$ ) and is a polyhedral set (i.e. is the intersection of  $\Omega$  with a finite union of  $N - 1$  dimensional simplexes) then (4.6) holds and thus by our preceding proof, the upper inequality holds. Next we invoke the density Theorem of Cortesani and Toader [16], that says that any function  $u \in SBV \cap L^\infty$  can be approximated by a sequence of functions  $u_k$  with polyhedral singular sets, in such a way that for any  $U$  compactly supported in  $\Omega$  it holds

$$\limsup_{k \rightarrow +\infty} \int_{\bar{U} \cap S_{u_k}} (1 + |u_k^+ - u_k^-|) d\mathcal{H}^{N-1} \leq \int_{\bar{U} \cap S_u} (1 + |u^+ - u^-|) d\mathcal{H}^{N-1}.$$

This is enough to conclude the proof, using a further diagonal argument.  $\square$

## 5 The one-dimensional case

In order to discuss the main characteristics of the approach, we now consider the one-dimensional version of the model described in Section 3. In this case,  $\Omega$  is the rectangle  $\Omega \equiv \{(x_1, x_2) : -a/2 < x_1 < a/2, -b/2 < x_2 < b/2\}$ , with Dirichlet boundary  $\partial\Omega^D = \{-a/2 < x_1 < a/2, x_2 = \pm b/2\}$  and Neumann boundary  $\partial\Omega^N = \{x_1 = \pm a/2, -b/2 < x_2 < b/2\}$ .

Because of the symmetry of the problem, we assume that  $\partial_2 u \equiv 0$  and  $\partial_2 s \equiv 0$ , i.e.,  $u$  and  $s$  are functions of  $x_1$  only. Consequently, the slip surfaces are planes orthogonal to the  $x_1$  axis. For convenience of notation, we define  $u' := \partial_1 u$ ,  $s' := \partial_1 s$  so that, calling  $x := x_1$ , the problem is set in the interval  $I \equiv \{x : -a/2 < x < a/2\}$ . Moreover, for the jump points we fix the natural orientation that implies for any  $x \in J_u$ ,  $u^+ = u(x^+)$  and  $u^- = u(x^-)$ , so that  $(u^+ - u^-)(x) = u(x^+) - u(x^-) =: [u](x)$ . For simplicity we assume that there is no constraint *à la* Winkler, i.e.,  $\bar{\kappa} \equiv 0$  and, without loosing generality, we set  $b = 1$ .

Therefore, in the 1-D case the functional (3.1) becomes

$${}^1d\Pi(u) := \frac{1}{2}\mu \int_{I \setminus J_u} |u'|^2 dx + \sum_{x \in J_u} (\gamma + \sigma_0 |[u](x)|), \quad (5.1)$$

whose minimizers have to be sought in the proper counterpart of the class of admissible functions (3.2) defined<sup>5</sup> as

$$\mathcal{A}^{1d} = \{u \in SBV(I, \mathbb{R}) ; u(-a/2) = -\beta a/2, u(a/2) = \beta a/2\} , \quad (5.2)$$

where  $\beta$  represents the average elongation.

On the other hand the regularized functional (3.4) takes the form

$${}^{1d}\Pi_\varepsilon(u, s) = \frac{1}{2}\mu \int_I (s^2 + o_\varepsilon)|u'|^2 dx + \gamma \int_I \left[ \varepsilon |s'|^2 + \frac{(1-s)^2}{4\varepsilon} \right] dx + \sigma_0 \int_I (1-s)^2 |u'| dx , \quad (5.3)$$

and the class of admissible functions (3.6) becomes

$$\hat{\mathcal{A}}^{1d} = \{(u, s) \in W^{1,2}(I, \mathbb{R}) \times W^{1,2}(I, \mathbb{R}) ; u(\pm a/2) = \pm \beta a/2, s(\pm a/2) = 1\} . \quad (5.4)$$

In the following, we will consider the response obtainable with the free-discontinuity functional and its regularized approximation and we will make comparisons between the two approaches.

### 5.1 The free-discontinuity problem

The minimization of functionals of the type of (5.1) in the class (5.2) has been considered by a number of authors, but now we are interested in the evolution problem as stated in Section 3.4. Therefore, we think of a loading history where  $\beta = \beta(t)$ ,  $t \in [0, T]$  for which we introduce the partition  $0, \dots, t_i, \dots, t_p \equiv T$ ,  $1 \leq i \leq p$ . By setting  $\beta_i = \beta(t_i)$  we define

$$\mathcal{A}_i^{1d} = \{u \in SBV(I, \mathbb{R}) ; u(\pm a/2) = \pm \beta_i a/2\} . \quad (5.5)$$

Let then  $u_i$  represent the solution of the evolution problem at the  $i$ th step. The solution  $u_{i+1}$  at step  $i+1$  is associated with the minimization problem

$$\min_{u \in \mathcal{K}_{i+1}} {}^{1d}\Pi^i(u) , \quad {}^{1d}\Pi^i(u) = \frac{1}{2}\mu \int_{I \setminus J_u} |u'|^2 dx + \sum_{x \in J_u} \{\gamma + \sigma_0 (|[u] - [u_i]| + |[u_i]|)\} . \quad (5.6)$$

where  $\mathcal{K}_{i+1}$  has been defined in (3.9). In the considerations which follow we will make extensive use of arguments similar to those of [25, Sect.3].

We first prove the following

**Proposition 3.** *For any  $i \in [1, p]$  the field  $u_i$  has at most one jump point, which for  $i \in [2, p]$ , coincides with the jump point of  $u_{i-1}$ , if any.*

<sup>5</sup>To be precise, one should define also for the 1-D case the counterpart of the relaxed problem (3.3), but for simplicity of analysis we will assume that the distinction is understood.

*Proof.* We first show that  $u_1$  has at most one jump point. In fact let  $\{x_k\}$ ,  $k = 1, \dots, n$  be the set of points  $x$  where  $[u_1](x) \neq 0$ . Consider, as an admissible variation, the function  $\eta$  such that  $J_\eta \equiv J_{u_1}$ ,  $\eta' \equiv 0$  and

$$[\eta](x_k) = -[u_1](x_k) \text{ for } k = 2, \dots, n \text{ and } [\eta](x_1) = -\sum_{k=2}^n [\eta](x_k). \quad (5.7)$$

We then obtain, since by construction  $[u_1 + \eta](x_k) = 0$  for all  $k \in [2, n]$ ,

$$\begin{aligned} {}^{1d}\Pi(u_1 + \eta) - {}^{1d}\Pi(u_1) &= \gamma + \sigma_0 |[u_1 + \eta](x_1)| - n\gamma - \sigma_0 \left( \sum_{k=1}^n |[u_1](x_k)| \right) \\ &= (1 - n)\gamma + \sigma_0 \left| [u_1](x_1) - \sum_{k=2}^n [u_1](x_k) \right| - \sigma_0 \left( \sum_{k=1}^n |[u_1](x_k)| \right) \leq (1 - n)\gamma, \end{aligned}$$

which proves that  $u_1$  cannot be a minimizer if  $n > 1$ . The same argument proves that if  $J_{u_i} = \emptyset$  then  $J_{u_{i+1}}$  has at most one jump point.

Now, if  $u_i$  has exactly one jump point at, say  $x = x_1$ , because of the definition of  $\mathcal{K}_{i+1}$  (3.9) then  $u_{i+1}$  has at least a jump at  $x = x_1$ . Consider, as before, the variation  $\eta$  such that  $J_\eta \equiv J_{u_{i+1}}$ ,  $\eta' \equiv 0$  and satisfies (5.7). We then have

$$\begin{aligned} {}^{1d}\Pi(u_{i+1} + \eta) - {}^{1d}\Pi(u_{i+1}) &= \sum_{x \in J_{u_{i+1} + \eta}} (\gamma + \sigma_0 |[u_{i+1} - u_i]|) - \sum_{x \in J_{u_{i+1}}} (\gamma + \sigma_0 |[u_{i+1} - u_i]|) \\ &= \gamma(1 - n) + \sigma_0 |[u_{i+1}](x_1) - [u_i](x_1) - \sum_{k=2}^n [u_i](x_k)| \\ &\quad - \sigma_0 |[u_{i+1}](x_1) - u_i(x_1)| - \sum_{k=2}^n |[u_{i+1}]| \\ &\leq \gamma(1 - n) \end{aligned}$$

which again proves that  $n = 1$ , and therefore at each step the number of jumps cannot exceed the unit.  $\square$

Observe that the field  $u_{i+1}$  must satisfy the first variation condition

$$\lim_{\lambda \rightarrow 0^+} \frac{1}{\lambda} \left( {}^{1d}\Pi^i[u_{i+1} + \lambda\eta] - {}^{1d}\Pi^i[u_{i+1}] \right) \geq 0, \quad (5.8)$$

for any variation  $u_{i+1} + \lambda\eta \in \mathcal{A}_{i+1}^{1d}$ , in particular satisfying

$$\int_{I \setminus J_\eta} \eta' dx + \sum_{x \in J_\eta} [\eta] = 0. \quad (5.9)$$

By taking different-in-type perturbations, one can prove the following

**Proposition 4.** *At each step  $i$ , we have that  $\mu u'_{i+1}$  is a constant, denoted  $\sigma \in [-\sigma_0, \sigma_0]$ . Moreover, if  $u_i$  has a jump at  $x = x_1$  and if  $\Delta := [u_{i+1}](x_1) - [u_i](x_1) \neq 0$  then*

$$\sigma = \text{sign}(\Delta)\sigma_0. \quad (5.10)$$

*Proof.* In (5.8) take a perturbation such that  $J_\eta = \emptyset$ . Then, one finds that  $u''_{i+1} = 0$  outside its jump, thus  $\mu u'_{i+1} =: \sigma$  is a constant.

From Proposition 3,  $u_{i+1}$  can have at most one jump point, say  $x_1$ , coinciding with the jump point of  $u_i$ . Now take a perturbation with constant  $\eta'$  and with a single jump  $[\eta]$  so that (5.9) implies  $a\eta' + [\eta] = 0$ . Now as in [25, Proposition 3.1], using the inequality  $|a + b| - |b| \leq |a|$  one finds that

$$\begin{aligned} 0 &\leq {}^{1d}\Pi^i[u_{i+i} + \lambda\eta] - {}^{1d}\Pi^i[u_{i+i}] \\ &= \sigma_0 (|[u_{i+1}] - [u_i] + \lambda[\eta]| - |[u_{i+1}] - [u_i]|) - \mu u'_{i+1} \lambda[\eta] + o(\lambda) \\ &\leq \sigma_0 |\lambda[\eta]| - \mu u'_{i+1} \lambda[\eta] + o(\lambda). \end{aligned} \quad (5.11)$$

Dividing first by  $|\lambda[\eta]|$  and passing to the limit we obtain  $\sigma \leq \sigma_0$ , and then dividing by  $-|\lambda[\eta]|$  we obtain the reverse inequality so that  $\sigma \in [-\sigma_0, \sigma_0]$ .

Now we assume that  $[u_{i+1}] - [u_i] \neq 0$ . Since  $|t'| = \text{sign}(t)$  for all  $t \neq 0$ , returning to (5.11) we obtain that

$$0 \leq \sigma_0 \text{sign}([u_{i+1}] - [u_i])\lambda[\eta] - \mu u'_{i+1} \lambda[\eta] + o(\lambda),$$

Dividing by  $\lambda[\eta]$  and  $-\lambda[\eta]$  and passing to the limit, one obtains

$$\sigma_0 \text{sign}([u_{i+1}] - [u_i]) - \mu u'_{i+1} = 0$$

which ends the proof of the Proposition.  $\square$

The quantity  $\sigma$  represents the shear stress in the body. In other words, the significance of Proposition 4 is that an increase (decrease) in the plastic slip can only occur where the shear stress  $\sigma$  equals  $\sigma_0$  ( $-\sigma_0$ ), whereas no plastic slip occurs when  $|\sigma| < \sigma_0$ . These are the usual assumptions of perfect plasticity.

In conclusion, there are only two possible states for the body: either the *unyielded* (elastic) state, where the displacement field is continuous, or the *yielded* (overstrained) state, where the plastic part of the deformation localizes in one shear band, associated with the point of discontinuity of the corresponding displacement field.

Suppose that the load history is such that  $\beta = \beta(t)$  is monotonically increasing from  $\beta = 0$ . There will be a certain threshold  $\beta = \beta_0 > 0$  that marks a transition from the unyielded to the yielded state. In the unyielded state, from Proposition 4 we have that  $u'$  is a constant, and  $u' = \sigma/\mu = \beta$ . Consequently the strain energy (5.1) reads

$${}^{1d}\Pi_e = \frac{1}{2} \mu a \beta^2. \quad (5.12)$$

On the other hand, from proposition 3 in the yielded state the displacement field has at most one jump at, say,  $x = x_1$  and, from Proposition 4,  $\sigma = \sigma_0$ . In the elastic part, one

still has that  $u'$  is constant, equal now to  $\sigma_0/\mu$  so that  $a\beta = a\sigma_0/\mu + [u](x_1)$ . Using this expression, the strain energy (5.1) takes the form

$${}^1d\Pi_y = \frac{1}{2} \frac{\sigma_0^2}{\mu} a + \gamma + \sigma_0[u] = \gamma + a\beta\sigma_0 - \frac{1}{2} \frac{\sigma_0^2}{\mu} a. \quad (5.13)$$

At the critical value  $\beta = \beta_0$  the two expressions (5.12) and (5.13) must be equal. We then obtain the following 2nd order equation in  $\beta$

$$\beta^2 - \beta \frac{2\sigma_0\beta}{\mu} + \left( \frac{\sigma_0^2}{\mu^2} - \frac{2\gamma}{\mu a} \right) = 0.$$

This equation has always two solutions of which only one is nonnegative, namely

$$\beta_0 = \frac{\sigma_0}{\mu} + 2\sqrt{\frac{2\gamma}{a\mu}}. \quad (5.14)$$

It is interesting for us to follow a strain driven test in which  $\beta$  undergoes the following time history:

**Step 1:**  $\beta$  is gradually augmented from the null value up to  $\beta_1 > \beta_0$ ;

**Step 2:**  $\beta$  is successively diminished from  $\beta_1$  to  $\beta_2 < (\beta_1 - 2\sigma_0/\mu)$ ;

**Step 3:**  $\beta$  is further increased from  $\beta_2$  to  $\beta_3 > (\beta_2 + 2\sigma_0/\mu)$ .

**Step 4:** The body is released so that  $\sigma = 0$ .

The response can be summarized in the graph of figure 5 representing the shear stress  $\sigma \equiv \mu u'$  as a function of the shear strain  $\beta$ . At first the response is linear elastic in the branch  $O \rightarrow A$  in fig. 5. At  $\beta = \beta_0$  of (5.14) there is the transition from the unyielded to the yielded state, and the stress  $\sigma$  drops from the value  $\sigma = \mu\beta_0$  at point  $A$  to the value  $\sigma_0$  at point  $A'$ . This is a very well-known phenomenon in the yielding of mild steel: after C. von Bach ([39, Section 19.1]), point  $A$  is traditionally called the upper-yield point (*Oberestreckgrenze*) and  $A'$  the lower-yield point (*Untereestreckgrenze*). The physical reasons of this stress drop consists in the phenomenon of the unpinning of the dislocations, already discussed in Section (3.2). When  $\beta > \beta_0$  the body is in the yielded state, and this condition is such that  $\Delta > 0$  in (5.10) of Proposition 4, so that  $\sigma$  is a constant and equal to  $\sigma_0$ .

At  $\beta = \beta_1$  the specimen is released. Now we have that the parameter  $\Delta$  of proposition 4 is such that  $\Delta = 0$ , that is, no plastic deformation occurs and the response is completely elastic. The representative point in the graph of fig. 5 follows the linear path  $B \rightarrow C$ . It is worth mentioning that if at some point, say  $B'$ , of the branch  $B - C$  the specimen is reloaded, the representative point would follow the path  $B' \rightarrow B \rightarrow B''$ , i.e., there is no distinction between the upper and lower-yield points when the specimen is released and successively reloaded. In the model, this is because the energy  $\gamma$  has already been paid to open the possibility of plastic slip. This finding is corroborated by the experimental

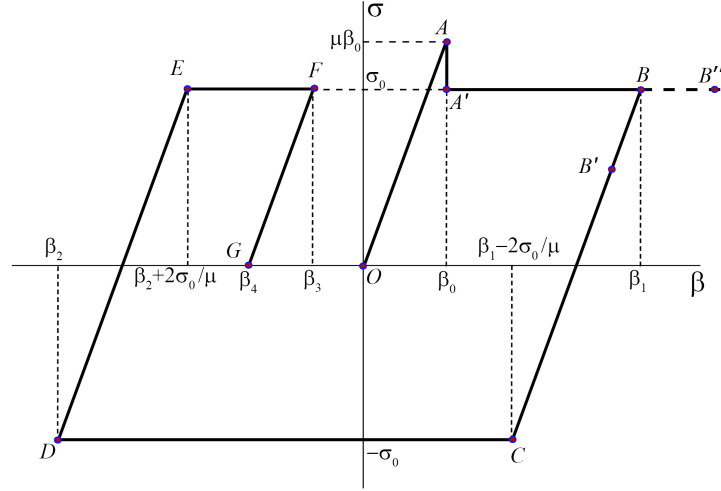


Figure 5: Shear stress  $\sigma$  vs. shear strain  $\beta$  in a strain-driven test where  $\beta$  follows the path  $0 \rightarrow \beta_1 \rightarrow \beta_2 \rightarrow \beta_3 \rightarrow \beta_4$ .

evidence [31] because once the dislocation has been unpinned, plastic flow can occur at constant stress in the representative slip plane.

At point  $C$ , where  $\beta = \beta_1 - 2\sigma_0/\mu$ , the model is a condition where, if  $\beta$  is further diminished,  $\Delta < 0$  in (5.10) of Proposition 4, so that  $\sigma = -\sigma_0$ . At point  $D$  where  $\beta = \beta_2$  the strain is further augmented and the condition is again such that  $\Delta = 0$  in Proposition 4, so that the representative point in the graph follows the linear elastic path  $D \rightarrow E$ . At  $E$ , where  $\beta = \beta_2 + 2\sigma_0/\mu$  the condition is again such that  $\Delta > 0$  in (5.10) of Proposition 4 and  $\sigma = \sigma_0$ . Finally at point  $F$  the specimen is further released: the representative point follows the linear path  $F \rightarrow G$  where, at  $G$ ,  $\sigma = 0$ . It is worth emphasizing that the permanent plastic strain  $\beta_4 = \beta_3 - \sigma_0/\mu$  remains stored in the body.

## 5.2 The regularized problem

A complete analysis of the regularized model goes beyond the scope of this paper because it necessitates of an *ad hoc* numerical code that will be the subject of further work. Here we limit just to discuss some qualitative aspects of the model, focusing the attention on the first onset of plastic deformations, that is on the counterpart, for the case of the regularized problem, of the branch  $O \rightarrow A \rightarrow A' \rightarrow B$  of Fig. 5. In other words, the problem can be associated with the very first step  $0 \leq t \leq t_1$  of the evolution problem outlined in (3.11)-(3.12)-(3.13): consequently, we will consider directly the minimization of the functional  ${}^{1d}\Pi_\varepsilon(u, s)$  of (5.3) in the class of admissible functions  $\hat{\mathcal{A}}^{1d}$  of (5.4).

Any equilibrium solution of this problem needs to satisfy the Euler equations, that for the case at hand, follow from condition

$$\lim_{\lambda \rightarrow 0^+} \frac{1}{\lambda} \left( {}^{1d}\Pi_\varepsilon(u + \lambda\eta, s + \lambda\varphi) - {}^{1d}\Pi_\varepsilon(u, s) \right) \geq 0, \quad (5.15)$$

Taking a variation  $u + t\eta$  of  $u$  with  $s$  fixed ( $\varphi = 0$ ) and  $\eta$  supported in a small enough neighborhood of a point  $x$  and, successively, taking a variation  $s + t\varphi$  of  $s$  with  $u$  fixed ( $\eta = 0$ ), one finds the conditions

$$\begin{cases} \sigma' = 0, \\ S' - T = 0, \end{cases} \quad (5.16)$$

where

$$\begin{aligned} \sigma &:= \mu(s^2 + o_\varepsilon)u' + \sigma_0(1-s)^2 \frac{u'}{|u'|}, \\ T &:= \mu s(u')^2 - (1-s)\left(\frac{\gamma}{4\varepsilon} + \sigma_0|u'|\right), \\ S &= 2\gamma\varepsilon s'. \end{aligned} \quad (5.17)$$

Observe that the first equation of (5.16) is valid only at points  $x$  such that  $u'(x) \neq 0$ , while the second one of (5.16) is valid everywhere.

According to a procedure already established by many authors (see e.g. [4, Sect. 4.4]), we first consider a stability analysis where a solution of the Euler equation is searched in the class

$$\tilde{\mathcal{A}}^{1d} = \{(u, s) \in C^2(I, \mathbb{R}) \times C^2(I, \mathbb{R}) ; u(\pm a) = \pm\beta a, s'(\pm a) = 0\}. \quad (5.18)$$

Clearly, the only difference with the class  $\hat{\mathcal{A}}^{1d}$  of (5.4) consists in the boundary conditions for  $s$  at the extremities and in the regularity assumption. The convenience of this choice is that now the homogeneous field  $(u, s)$  with  $u'$  identically constant and  $s$  identically constant are solutions of the Euler equations with

$$u(x) = \beta x, \quad s(x) = \frac{\frac{\gamma}{4\varepsilon} + \sigma_0|\beta|}{\mu\beta^2 + \frac{\gamma}{4\varepsilon} + \sigma_0|\beta|}. \quad (5.19)$$

Figure 6 shows the solution for a paradigmatic case for which  $\mu = 100$  GPa,  $\sigma_0 = 10^{-3}\mu$ ,  $\gamma = 0.25a\sigma_0^2/\mu$ , so that in (5.14),  $4(\gamma/a\mu) = 0.25(\sigma_0/\mu)^2$ . In particular, fig. 6(a) shows the stress  $\sigma$  of (5.17)<sub>1</sub> as a function of the average shear strain  $\beta$  and the regularized parameter  $\varepsilon$  in representative intervals. There are various curves on the plotted surface. The curves referred to as “ $\beta = \sigma_0/\mu$ ”, “ $\sigma = \sigma_0$ ” and “ $\sigma = \mu\beta_0$ ” represent, respectively, the intersection of the  $\sigma$ - surface with the planes  $\beta = \sigma_0/\mu$ ,  $\sigma = \sigma_0$  and  $\sigma = \mu\beta_0$ , where  $\beta_0$  is given in (5.14). On the same figure we have represented, with dashed lines, the intersection of the surfaces with planes  $\varepsilon = \text{const.}$ , each plane spaced at an interval  $\Delta\varepsilon = 0.25 \times 10^{-3}a$ .

The analysis of the second variation for the problem at hand gives the necessary condition

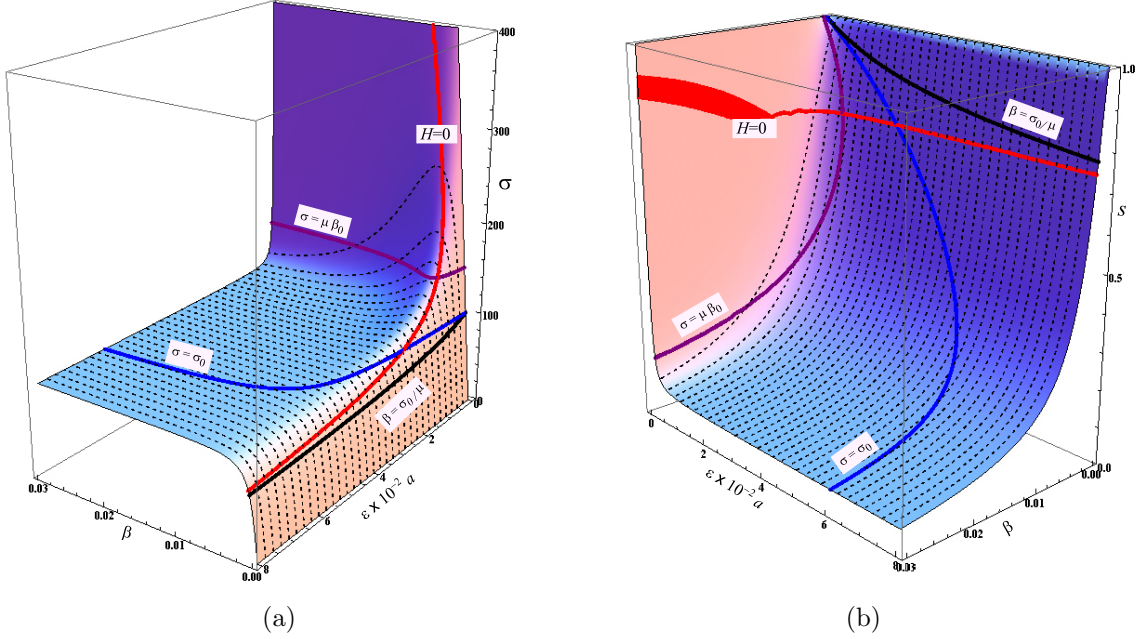


Figure 6: a) Shear stress  $\sigma$  as a function of average shear strain  $\beta$  and regularization parameter  $\varepsilon$ ; b) Field  $s$  as a function of  $\beta$  and  $\varepsilon$ .

$$H := \partial_{u'} \sigma \partial_s S - (\partial_s \sigma)^2 > 0. \quad (5.20)$$

This condition gives restrictions of the values of  $\beta$  and  $\varepsilon$  that correspond to “locally” stable solutions. In particular on the  $\sigma$ – surface of fig. 6(a) we have plotted the curve labeled “ $H = 0$ ”, corresponding to condition  $H = 0$  that represents the threshold of transition from a stable to an unstable solution.

In figure fig. 6(b) we have drawn the surface associated with field  $s$ , again as a function of  $\beta$  and  $\varepsilon$ , with the sections  $\varepsilon = \text{const.}$ , spaced an interval  $\Delta\varepsilon = 0.25 \times 10^{-3}a$ , and corresponding counterparts of the curves “ $\beta = \sigma_0/\mu$ ”, “ $\sigma = \sigma_0$ ”, “ $\sigma = \mu\beta_0$ ” and “ $H = 0$ ”.

Various peculiarities can be distinguished.

- i)* There is not a purely elastic phase with  $s = 1$  because, from (5.19),  $s < 1$  whatever small the parameter  $\beta$  is (a purely elastic phase can only be attained as  $\varepsilon \rightarrow 0$ ). The material is softer than a purely elastic phase because in fig. 6(a) the curve “ $\beta = \sigma_0/\mu$ ” is always lower than the curve “ $\sigma = \sigma_0$ ”, but the two curves tend to coincide when  $\varepsilon \rightarrow 0$ .
- ii)* Considering the stress-strain relationships of fig. 6(a) at constant  $\varepsilon$ , one can notice that for small  $\varepsilon$  the corresponding response presents a strain-softening phase, whereas the relationship is monotone increasing for sufficiently large  $\varepsilon$ . It is also evident from fig.

- 6(b) that the corresponding  $s$  is always monotone decreasing. Moreover,  $\sigma \rightarrow \sigma_0$  for  $\beta$  sufficiently large.
- iii)* The curve “ $H = 0$ ” marks the beginning of the instability of the homogeneous solution (5.19). The corresponding critical value of  $\sigma$ , say  $\sigma_c$ , increases with decreasing  $\varepsilon$  and  $\sigma_c \rightarrow +\infty$  as  $\varepsilon \rightarrow 0$ .
- iv)* There are values of  $\varepsilon$ , say  $\varepsilon_1$  and  $\varepsilon_2 > \varepsilon_1$ , such that  $\sigma_c < \sigma_0$  for  $\varepsilon_2 < \varepsilon$ ,  $\sigma_0 < \sigma_c < \mu\beta_0$  for  $\varepsilon_1 < \varepsilon < \varepsilon_2$  and  $\mu\beta_0 < \sigma_c$  for  $0 < \varepsilon < \varepsilon_1$ .

The property *i)* is in agreement with what already observed in [4, Section 4.4.], for a fracture model *à la* Griffith, with no plastic phase. Moreover, the fact that  $\sigma_c$ , increases as  $\varepsilon$  decreases, as stated in *iii)*, has been commented in [10] for the simplest 1D fracture model *à la* Griffith. The reason for this is that solutions of the Euler equations (5.16), which also satisfy the second variation conditions (5.20), are equilibrium configurations that not necessarily correspond to *global* minima. The  $\Gamma$ -convergence result of Section 4 is thus not in contrast with the analysis of Section 5.1 because the mathematical theory only assures convergence of global minimizers and the corresponding minima. In Section 5.1 we had observed an upper bound for the shear stress equal to  $\sigma = \mu\beta_0$ , with  $\beta_0$  given by (5.14), and the analysis which has led to the result summarized in Figure 5 was based upon global minimization of the free discontinuity functional (5.6). Indeed, as discussed at length by Del Piero and Truskinovsky, if one considers, as in [25, Section 3.2], the natural metric of *SBV* to attribute a finite distance to configurations with different jump sets, one finds that all equilibrium configuration without jumps are locally stable ([25, Corollary 3.4]). In other words, as already noticed by Marigo *et al.* [15], the free-discontinuity formulation presents the drawback that if local minima are looked for, the load required to open a crack is infinite. The counterpart of this finding in the regularized model at hand is that  $\sigma_c \rightarrow +\infty$  as  $\varepsilon \rightarrow 0$ .

We then pass to consider more in detail the regularized problem. Of particular importance is the following

**Proposition 5.** *Assume that  $u, s \in C^2(I)$ .*

- (i)* If  $\beta > 0$ , then  $u' \geq 0$  in  $I$  and there exists a constant  $\bar{\sigma}$ , with  $\bar{\sigma} > 0$ , such that

$$u'(x) = \frac{\max(0, \bar{\sigma} - \sigma_0(1 - s(x))^2)}{\mu(s^2(x) + o_\varepsilon)}, \quad \text{for all } x \in I \quad (5.21)$$

- (ii)* If  $\beta < 0$ , then  $u' \leq 0$  in  $I$  and there exists a constant  $\bar{\sigma}$ , with now  $\bar{\sigma} < 0$ , such that

$$u'(x) = \frac{\min(0, \bar{\sigma} + \sigma_0(1 - s(x))^2)}{\mu(s^2(x) + o_\varepsilon)}, \quad \forall x \in I \quad (5.22)$$

*Proof.* Since we assume  $u'$  to be continuous, the sets  $\Omega_+ := I \cap \{x; u'(x) > 0\}$  and  $\Omega_- := I \cap \{x; u'(x) < 0\}$  are open, while the set  $\Omega_0 := I \cap \{x; u'(x) = 0\}$  is closed. By (5.16) we

know that  $\mu(s^2 + o_\varepsilon)u' + \sigma_0(1 - s)^2$  is locally constant on  $\Omega_+$  and  $\mu(s^2 + o_\varepsilon)u' - \sigma_0(1 - s)^2$  is locally constant on  $\Omega_-$ . We claim that those constants actually do not depend on the connected components of  $\Omega_+$  or  $\Omega_-$ . To see this, let us take a smooth nonnegative function  $\zeta$  with compact support satisfying  $\int_{\mathbb{R}} \zeta(\tau) d\tau = 1$  and define  $\varphi_h(x)$  as being a primitive of  $x \mapsto h^{-1}\zeta(x/h)$ . In this way  $\varphi'_h(x)$  is a mollifier and in particular we have that  $\int_{\mathbb{R}} \varphi'_h(x) dx = 1$  for all  $h > 0$  whereas the size of the support of  $\varphi'_h$  becomes very small around the origin when  $h \rightarrow 0$ . Now, let  $x_1$  and  $x_2$  be two points situated in two different connected components of  $\Omega_+$ , and take as a variation for  $u$  the competitor

$$u_h := u(x) + t(\varphi_h(x - x_1) - \varphi_h(x - x_2)). \quad (5.23)$$

This is an admissible variation for  $h$  small enough because by construction

$$\int_I (\varphi_h(x - x_1) - \varphi_h(x - x_2))' dx = 0.$$

Now using that  $(u, s)$  is a minimizer and denoting  $\sigma_1 = \mu(s^2(x_1) + o_\varepsilon)u'(x_1) + \sigma_0(1 - s(x_1))^2$  and  $\sigma_2 = \mu(s^2(x_2) + o_\varepsilon)u'(x_2) + \sigma_0(1 - s(x_2))^2$  the constants associated with  $x_1$  and  $x_2$  we find that

$$\sigma_1 \int_I \varphi'_h(x - x_1) - \sigma_2 \int_I \varphi'_h(x - x_2) = \sigma_1 - \sigma_2 = 0$$

hence  $\mu(s^2 + o_\varepsilon)u' + \sigma_0(1 - s)^2$  is identically constant on  $\Omega_+$ , and we denote this constant by  $\sigma_+$ . The same argument shows that  $\mu(s^2 + o_\varepsilon)u' - \sigma_0(1 - s)^2$  is identically constant on  $\Omega_-$ , and we denote this constant by  $\sigma_-$ . We claim now that  $\sigma_+ = \sigma_-$ . Indeed, this can be seen as before using the variation (5.23) with now  $x_1 \in \Omega_+$  and  $x_2 \in \Omega_-$ . As a result there exists a constant  $\bar{\sigma}$  such that

$$u' = \frac{\bar{\sigma} - \sigma_0(1 - s)^2}{\mu(s^2 + o_\varepsilon)}, \quad \forall x \in \Omega_+ \quad \text{and} \quad u' = \frac{\bar{\sigma} + \sigma_0(1 - s)^2}{\mu(s^2 + o_\varepsilon)}, \quad \forall x \in \Omega_-. \quad (5.24)$$

Now, if  $\bar{\sigma} > 0$  then  $\Omega_- = \emptyset$  because, if this is not the case,  $u'$  cannot be negative in (5.24); *vice versa*, if  $\bar{\sigma} < 0$  then  $\Omega_+ = \emptyset$  otherwise  $u'$  cannot be positive in (5.24). But if  $\beta > 0$  one necessarily has  $\Omega_+ \neq \emptyset$  and consequently  $\bar{\sigma} > 0$ . On the other hand if  $\beta < 0$  then  $\Omega_- \neq \emptyset$  thus  $\bar{\sigma} < 0$ .

It remains to see what is happening on  $\Omega_0 := \{x ; u'(x) = 0\}$ . Without loss of generality we may assume now that  $\bar{\sigma}$  is positive, so that  $\Omega_- = \emptyset$ . The proof works by the same way with  $\bar{\sigma} < 0$ . To finish the proof of the proposition we have to show that  $\sigma_0(1 - s)^2 \geq \bar{\sigma}$  on  $\Omega_0$ . First notice that by continuity of  $s$  on  $I$  the equation (5.24) remains true on  $\bar{\Omega}_+$ , and in particular  $\sigma_0(1 - s)^2 = \bar{\sigma}$  on  $\partial\Omega_0$ . Now we take again the variation  $u_\varepsilon$  defined on (5.23) this last time with  $x_1$  lying in the interior of  $\Omega_0$  and  $x_2 \in I \setminus \Omega_0 = \Omega_+$ . The first order condition gives that

$$\int_I \sigma_0(1 - s)^2 |\varphi'_h(x - x_1)| dx - \int_I \bar{\sigma} \varphi'_h(x - x_2) dx \geq 0, \quad (5.25)$$

Since  $\varphi'_h$  is a nonnegative mollifier, taking the limit  $h \rightarrow 0$  one gets  $\sigma_0(1 - s(x))^2 \geq \bar{\sigma}$  for any  $x \in \Omega_0$ , which ends the proof of the Proposition.  $\square$

**Remark 3.** In practice, the counterpart for the regularized problem of proposition 4, valid for the free-discontinuity problem, is this proposition 5. Here  $\bar{\sigma}$  represents the shear stress in the body and the significance of the proposition is that, in order to produce plastic strain, this stress has to reach, in absolute value, a certain threshold associated with the value of the stress  $\sigma_0$ . In fact when  $|\bar{\sigma}|/\sigma_0 \ll 1$  we find that at points where  $s \rightarrow 0$  (yielded material) we would have  $u' = 0$ . This conclusion should be associated with that of proposition 4 according to which the plastic slip, represented by the jump of the displacement field, is null whenever the shear stress is, in absolute value, less than  $\sigma_0$ .

To discuss further the qualitative features of the regularized model, we consider a particular field

$$s = 1 - e^{-\frac{1}{2}x/\varepsilon}. \quad (5.26)$$

This choice as discussed, e.g., in [11] and [37], has the advantage that it provides a lower bound for the second integral on the r.h.s. of (5.3) when the interval  $I$  is infinite. For the case at hand, we easily find

$$\int_I \varepsilon (s')^2 + \frac{(1-s)^2}{4\varepsilon} dx = 1 - e^{-a/\varepsilon}, \quad (5.27)$$

which clearly tends to 1 as  $a \rightarrow \infty$ . This choice wants to simulate the occurrence of one slip plane at  $x = 0$ . Substituting  $s$  into (5.21), one finds the corresponding shear strain  $u'$  as a function of the shear stress  $\sigma$  and, once these fields are given, corresponding energy  ${}^{1d}\Pi_\varepsilon(u, s)$  of (5.3) can be evaluated.

An energetic competition is thus engaged between this solution, which now represents the counterpart of the solution with one slip point of section 5.1, and the energy corresponding to the homogeneous solution (5.19). The two graphs corresponding to the aforementioned solutions, labeled “homogeneous” and “1-slip”, are juxtaposed in Figure 7.

The plots correspond to the same material parameters of the graphs of figure 6 but, here, they are represented as a function of the shear stress  $\sigma$  and the order parameter  $\varepsilon$ . The intersection between the two graphs mark the transition to a case in which the “1-slip” solution becomes energetically favorable with respect to the “homogeneous” solution.

Examining first the “homogeneous” surface, it should be noticed that this is anticlástico bent so that, for any fixed  $\varepsilon$  there is in general a maximal stress that can be supported by the body. Such stress practically coincides, in the assumed interval of  $\varepsilon$  with the stress  $\sigma_c$  identified in figure 6 by the curve “H=0”. On the other hand the “1-slip” surface is monotonically increasing with  $\sigma$  and exhibits only a slight dependence upon  $\varepsilon$ . Such energy surface asymptotically tends to an inclined plane as  $\sigma \rightarrow \infty$  due to the linear dependence of  ${}^{1d}\Pi_\varepsilon(u, s)$  of (5.3) upon  $|u'|$ .

Observe that for any fixed  $\varepsilon$  the intersection between the two curves corresponds to a stress threshold far lower than the critical stress  $\sigma_c$  of figure 6 (curve “H=0”). This confirms that *global* minimizers correspond to energetic levels far below those associated with *local* minimizers. Of course, the “1-slip” surface has been obtained through the assumption that

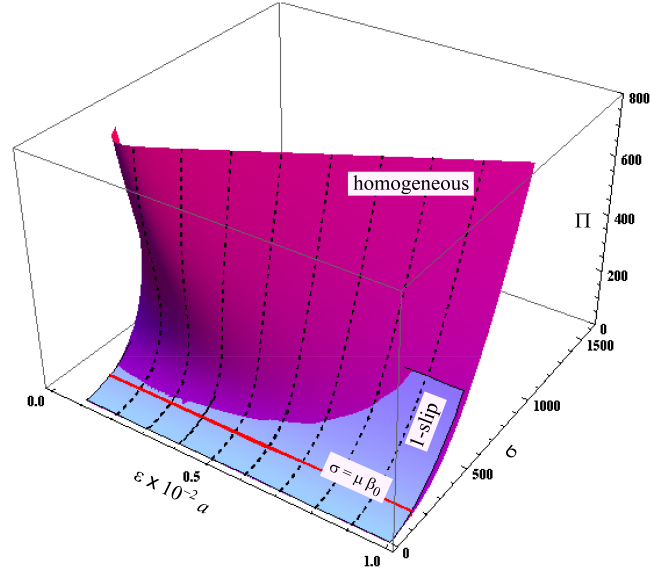


Figure 7: Strain energy for the regularized model as a function of shear stress  $\sigma$  and of the order parameter  $\varepsilon$ . Cases of “homogeneous” and “1-slip” solutions.

$s$  is of the form (5.26), but the surface corresponding to the *true* solution is certainly below this one. Consequently, the stress corresponding to the onset of one slip is certainly lower than the one that can be inferred from the intersection of the two surfaces plotted in figure 7. Last but not least, we notice that such critical value of the stress diminishes as  $\varepsilon$  decreases and, as evidenced in the figure, it is of the order of 150Mpa, which represents, for the case at hand, the value of  $\mu\beta_0$ , with  $\beta_0$  given by (5.14), associated with the *upper yield point* in figure 5.

## 6 Concluding remarks

Although this model is minimal and can be considered just a first attempt at describing the complex phenomenon of plastic flow, it highlights that the proposed variational approach seems to be quite promising. The mathematical setting in the space of *SBV* functions allows to account for the fact that the deformation of an elastic-plastic body is indeed *structured*, in the sense stated by Del Piero and Owen [24]. In fact, the plastic part of the deformation is due to slips that can be modeled as jumps in the component of displacement tangential to the glide surface. The location of the slip surfaces does not need to be known *a priori*, but

can be found from the boundary data (*free-discontinuity* problem). Irreversibility of plastic flow can be considered by following the loading history through a sequence of minimization sub-problems associated with the incremental energy consumption.

The regularized approximation of the aforementioned free-discontinuity problem through a sequence of elliptic problems, labeled by the order parameter  $\varepsilon$  for  $\varepsilon \rightarrow 0$ , has various deep implications. First of all, the essence of the relationship between the regularized and the parent free-discontinuity models is mathematically made precise by the  $\Gamma$ -convergence result. On the one hand, the deformation field predicted by the regularized approach would represent a somehow smeared view of the phenomenon of plastic slips, showing strain localizations tending to sharp discontinuities as  $\varepsilon \rightarrow 0$ . But, indeed, the experimental evidence shows that the localization of plastic deformation occurs not along sharp interfaces, but in layers (bands) of very small but finite thickness [39]. Therefore, the regularized setting could be considered not just a mere approximation, but an autonomous model *per se* [37], lying in the class of the pseudo non-local *gradient-damage* models [30]. In particular, it physically interprets the phenomenon of localization of plastic flow due to coalescence of microvoids or microcracks, triggered by material inhomogeneities like notches or inclusions, that concentrate in slip layers whose thickness is identified by the parameter  $\varepsilon$ . Consequently, as discussed at length in [37],  $\varepsilon$  represents an important material parameter that is usually referred to as the *material intrinsic length scale*. According to this rationale, it is the free-discontinuity  $\Gamma$ -limit that represents an approximation of a more comprehensive model, obtained by letting the material intrinsic length scale go to zero. Since the setting of the free-discontinuity problem presents strict analogies with the propagation in mode II of cohesive fractures [43], the  $\Gamma$ -limit result establishes strict analogies between the theories of plasticity, cohesive fracture and damage, as inferred in [23] and somehow already stated in the famous approach by Hillerborg [35].

One of the main characteristics of the proposed model is that, in general, it may predict the extreme localization of the inelastic part of the deformation in *one* slip surface for the free-discontinuity problem or, equivalently, in *one* thin band for the regularized approximating problem. However, when plastic flow is somehow confined by neighboring parts of the body that remain elastic, the model may predict the *diffusion* of the plastic region in a bulk part of the body, as shown for a paradigmatic example in the numerical experiments presented in [29]. In this case, the model at hand could well reproduce the results of the classical theory of plasticity, where plastic deformation is a bulk phenomenon and plastic strains are represented by sufficiently regular fields. However, the tendency towards localization could also be a consequence of the minimality of the model, that certainly does not take into account at least two effects that appear fundamental [31] for the diffusion of plastic deformation: the phenomenon of strain hardening and the interaction between slip surfaces. By insight, a desirable improvement could be the consideration of more general forms of the energy functional associated with plastic flow through the introduction of a non-local spatial dependence for the strain variable as pursued, for example, in [22].

Last but not least, we have to mention that  $\Gamma$ -convergence deals with *global* minima and minimizers, whereas we have underlined in the 1-D example here presented that there are representative equilibrium solutions that are *locally*, though not globally, stable that can

be attained in a quasi-static loading history. For the case of brittle fracture, only recently the substantial difference between local and global minima, which has major consequences on the stage of crack initiation, has been recognized in [15] and specified [25] for a 1-D free-discontinuity model, while the local minimization of the regularized energies and its relationship with the parent problem has been explored, still for the 1-D case, in [10]. For the model at hand, we have tentatively shown in a particular example that there is some sort of relationship between local minimizers of free-discontinuity functional and of the regularized functional, although the approximating properties of the latter with respect to the former cannot be assured through  $\Gamma$ -convergence, which proves convergence of global minima only. This issue, as well as the extension of the  $\Gamma$ -convergence theory from the 2-D antiplane shear to more general cases of generalized plane stress or plane strain, needs to be clarified in further work.

### Acknowledgements

L.Am. gratefully acknowledges the support of the MIUR PRIN06 grant. G.R.C. would like to acknowledge the partial support of the Italian MURST under the PRIN-2008 program “Structural use of glass”. This work was done while A.Le. was affiliated to the mathematical research center E. De Giorgi and he wishes to thank all the members of the center and the Scuola Normale Superiore of Pisa for their kind hospitality.

### References

- [1] R. Alicandro, A. Braides, and J. Shah. Free-discontinuity problems via functionals involving the  $L^1$ -norm of the gradient and their approximations. *Interfaces Free Bound.*, 1(1):17–37, 1999.
- [2] L. Ambrosio, N. Fusco, and D. Pallara. *Functions of bounded variation and free discontinuity problems*. Oxford Mathematical Monographs. The Clarendon Press Oxford University Press, New York, 2000.
- [3] L. Ambrosio and V. M. Tortorelli. On the approximation of free discontinuity problems. *Boll. Un. Mat. Ital. B (7)*, 6(1):105–123, 1992.
- [4] H. Amor, J.-J. Marigo, and C. Maurini. Regularized formulation of the variational brittle fracture with unilateral contact: Numerical experiments. *Journal of the Mechanics and Physics of Solids*, 57(8):1209 – 1229, 2009.
- [5] R. J. Asaro and J. R. Rice. Strain localization in ductile single crystals. *Journal of the Mechanics and Physics of Solids*, 25(5):309 – 338, 1977.
- [6] A. Aydin and A. M. Johnson. Analysis of faulting in porous sandstones. *Journal of Structural Geology*, 5(1):19 – 31, 1983.

- 
- [7] G. I. Barenblatt. The mathematical theory of equilibrium cracks in brittle fracture. In *Advances in Applied Mechanics, Vol. 7*, pages 55–129. Academic Press, New York, 1962.
- [8] D. Bigoni and F. Dal Corso. The unrestrainable growth of a shear band in a prestressed material. *Proceedings of the Royal Society A: Mathematical, Physical and Engineering Science*, 464(2097):2365–2390, 2008.
- [9] L. Biolzi and G. Royer-Carfagni. Experimental evidence of serrated elastic-plastic deformation of metallic bars under torsion. In *Atti XV Congresso Nazionale AIMETA*, pages SPSO–04(in extenso on CD–ROM), Taormina, Italy, September 2001.
- [10] B. Bourdin. Numerical implementation of the variational formulation for quasi-static brittle fracture. *Interfaces Free Bound.*, 9(3):411–430, 2007.
- [11] B. Bourdin, G. A. Francfort, and J.-J. Marigo. Numerical experiments in revisited brittle fracture. *J. Mech. Phys. Solids*, 48(4):797–826, 2000.
- [12] A. Braides, A. Defranceschi, and E. Vitali. A relaxation approach to Hencky’s plasticity. *Appl. Math. Optim.*, 35(1):45–68, 1997.
- [13] A. Chambolle. A density result in two-dimensional linearized elasticity, and applications. *Arch. Ration. Mech. Anal.*, 167(3):211–233, 2003.
- [14] A. Chambolle. An approximation result for special functions with bounded deformation. *J. Math. Pures Appl. (9)*, 83(7):929–954, 2004.
- [15] M. Charlotte, J. Laverne, and J.-J. Marigo. Initiation of cracks with cohesive force models: a variational approach. *European Journal of Mechanics - A/Solids*, 25(4):649–669, 2006. 6th EUROMECH Solid Mechanics Conference - General/Plenary Lectures.
- [16] G. Cortesani and R. Toader. A density result in SBV with respect to non-isotropic energies. *Nonlinear Anal.*, 38(5, Ser. B: Real World Appl.):585–604, 1999.
- [17] A. Cottrell. *Dislocations and Plastic Flow in Crystals*. 4th ed. Clarendon Press, Oxford, 1961.
- [18] T. Cox and J. Low. An investigation of the plastic fracture of aisi 4340 and 18 nickel-200 grade maraging steels. *Metallurgical and Materials Transactions B*, 5:1457–1470, 1974. 10.1007/BF02646633.
- [19] G. Dal Maso. *An introduction to  $\Gamma$ -convergence*. Progress in Nonlinear Differential Equations and their Applications, 8. Birkhäuser Boston Inc., Boston, MA, 1993.
- [20] G. Dal Maso and R. Toader. A model for the quasi-static growth of brittle fractures: existence and approximation results. *Arch. Ration. Mech. Anal.*, 162(2):101–135, 2002.

- [21] E. De Giorgi and L. Ambrosio. New functionals in calculus of variations. In *Nonsmooth optimization and related topics (Erice, 1988)*, volume 43 of *Ettore Majorana Internat. Sci. Ser. Phys. Sci.*, pages 49–59. Plenum, New York, 1989.
- [22] C. De-Lellis and G. Royer-Carfagni. Interaction of fractures in tensile bars with non-local spatial dependence. *J. Elasticity*, 65(1-3):1–31 (2002), 2001.
- [23] G. Del Piero. Towards a unified approach to fracture yielding, and damage. In *Continuum models and discrete systems (Istanbul, 1998)*, pages 679–692. World Sci. Publ., River Edge, NJ, 1998.
- [24] G. Del Piero and D. R. Owen. Structured deformations of continua. *Arch. Rational Mech. Anal.*, 124(2):99–155, 1993.
- [25] G. Del Piero and L. Truskinovsky. Elastic bars with cohesive energy. *Continuum Mechanics and Thermodynamics*, 21(2):141 – 171, 2009.
- [26] D. S. Dugdale. Yielding of steel sheets containing slits. *Journal of the Mechanics and Physics of Solids*, 8(2):100 – 104, 1960.
- [27] M. Focardi. On the variational approximation of free-discontinuity problems in the vectorial case. *Math. Models Methods Appl. Sci.*, 11(4):663–684, 2001.
- [28] G. A. Francfort and J.-J. Marigo. Revisiting brittle fracture as an energy minimization problem. *J. Mech. Phys. Solids*, 46(8):1319–1342, 1998.
- [29] F. Freddi and G. Royer-Carfagni. A variational approach to plasticity. numerical experiments. In *Atti XX Congresso Nazionale AIMETA*, Bologna, Italy, September 2011.
- [30] M. Frémond. *Non-smooth Thermomechanics*. Heidelberg. Springer-Verlag, 2002.
- [31] M. Froli and G. Royer-Carfagni. A mechanical model for the elastic-plastic behavior of metallic bars. *International Journal of Solids and Structures*, 37(29):3901 – 3918, 2000.
- [32] V. Georgiannou. A laboratory study of slip surface formation in an intact natural stiff clay. *Géotechnique*, 56(8):551 – 559, 2006.
- [33] G. Hahn and A. Rosenfield. Metallurgical factors affecting fracture toughness of aluminum alloys. *Metallurgical and Materials Transactions A*, 6:653–668, 1975. 10.1007/BF02672285.
- [34] V. Hakim and A. Karma. Laws of crack motion and phase-field models of fracture. *Journal of the Mechanics and Physics of Solids*, 57(2):342 – 368, 2009.
- [35] A. Hillerborg, M. Modèer, and P. Petersson. Analysis of crack formation and crack growth in concrete by means of fracture mechanics and finite elements. *Cement and Concrete Research*, 6(6):773 – 781, 1976.

- [36] F. Körber and E. Siebel. Zur theorie der bildsamen formänderung. *Naturwissenschaften*, 16:408–412, 1928. 10.1007/BF01459027.
- [37] G. Lancioni and G. Royer-Carfagni. The variational approach to fracture mechanics. A practical application to the French *Panthéon* in Paris. *J. Elasticity*, 95(1-2):1–30, 2009.
- [38] L. D. Landau and E. M. Lifshitz. *The classical theory of fields*. Revised second edition. Course of Theoretical Physics, Vol. 2. Translated from the Russian by Morton Hamermesh. Pergamon Press, Oxford, 1962.
- [39] A. Nadai. *Theory of flow and Fracture of Solids*. McGraw-Hill. New York, 1950.
- [40] F. Nakanishi. On yield point of mild steel. *Report of the Aeronautical Research Institute*, 6:83 – 140, 1931.
- [41] A. Ord, I. Vardoulakis, and R. Kajewski. Shear band formation in gosford sandstone. *International Journal of Rock Mechanics and Mining Sciences and Geomechanics Abstracts*, 28(5):397 – 409, 1991.
- [42] K. Osakada. History of plasticity and metal forming analysis. *Journal of Materials Processing Technology*, 210(11):1436 – 1454, 2010.
- [43] A. C. Palmer and J. R. Rice. The growth of slip surfaces in the progressive failure of over-consolidated clay. *Proceedings of the Royal Society of London. A. Mathematical and Physical Sciences*, 332(1591):527–548, 1973.
- [44] R. Price and A. Kelly. Deformation of age-hardened aluminium alloy crystals–ii. fracture. *Acta Metallurgica*, 12(9):979 – 992, 1964.
- [45] J. R. Rice. The localization of plastic deformation. In W. Koiter, editor, *Theoretical and Applied Mechanics (Proceedings of the 14th International Congress on Theoretical and Applied Mechanics)*, pages 207 – 220, Delft, 1976. NorthHolland Publishing Co.
- [46] D. Rittel, Z. G. Wang, and M. Merzer. Adiabatic shear failure and dynamic stored energy of cold work. *Phys. Rev. Lett.*, 96(7):075502, Feb 2006.
- [47] E. Saurer and A. M. Puzrin. Energy balance approach to shear band propagation in shearblade tests. In *International Conference of International Association for Computer Methods and Advances in Geomechanics (IACMAG)*, pages 1024–1031, Goa, India, September 2008.
- [48] E. Saurer and A. M. Puzrin. Validation of the energy-balance approach to curve-shaped shear-band propagation in soil. *Proceedings of the Royal Society A: Mathematical, Physical and Engineering Science*, 467(2127):627–652, 2011.

- [49] K. Tanaka and J. Spretnak. An analysis of plastic instability in pure shear in high strength aisi 4340 steel. *Metallurgical and Materials Transactions B*, 4:443–454, 1973. 10.1007/BF02648697.
- [50] A. I. Vol’pert. Spaces BV and quasilinear equations. *Mat. Sb. (N.S.)*, 73 (115):255–302, 1967.
- [51] A. I. Vol’pert. Analysis in classes of discontinuous functions and partial differential equations. In *New results in operator theory and its applications*, volume 98 of *Oper. Theory Adv. Appl.*, pages 230–248. Birkhäuser, Basel, 1997.
- [52] E. Wessels and P. Jackson. Latent hardening in copper-aluminium alloys. *Acta Metallurgica*, 17(3):241 – 248, 1969.
- [53] H. Wolf, D. Knig, and T. Triantafyllidis. Experimental investigation of shear band patterns in granular material. *Journal of Structural Geology*, 25(8):1229 – 1240, 2003.